Thermal Degradation and Corrosion of Amines for CO$_2$ Capture

By:

Daniel Hatchell

Hanbi Liu

Omkar Namjoshi

Gary T. Rochelle

Chemical Engineering 679

McKetta Department of Chemical Engineering

Cockrell School of Engineering

The University of Texas

May 2015

Acknowledgements

I would like to thank Gary T. Rochelle for his assistance and guidance during my two years of undergraduate research. He has been kind, welcoming, and supportive of me as I slowly but surely learned the literature and experimental techniques behind carbon capture research. His enthusiasm and wisdom have strongly influenced me to attend graduate school.

I also want to give special thanks to Omkar Namjoshi, an outstanding mentor, teacher, and friend. I could not have completed the following work without his tireless and determined support. He is the model of what I hope to be if I ever have the opportunity to mentor an undergraduate student in my graduate career.

I want to thank my friend Hanbi Liu, an outstanding research partner that I have had the pleasure to work with these past two years. Her cheerful nature and outdated taste in music have made even the longest series of dilutions enjoyable. I wish her the greatest success after graduation.

I would like to give thanks to the members of the Rochelle group that have helped me throughout my undergraduate career. I give special mention to Maeve Cooney, Kent Fischer, Nathan Fine, Paul Nielsen, Yang Du, Peter Frailie, Nina Salta, and Verbin Sapkota. Every member of the group has helped me these past two years and I have enjoyed working with each of them.

I want to thank Matthew Carlson and Sovik De Sirkar, my two senior lab partners, who helped me struggle through countless amine samples used for corrosion measurements. I hope they know how helpful they have been towards completing this work.

I want to acknowledge the Texas Carbon Management Program for financial support for this research, without which the following work would not have been possible.

I finally want to sincerely thank my family and friends, without whom I would not have gotten to where I am today. My parents have encouraged me throughout college and very positively shaped my academic goals; my friends have kept me motivated and focused throughout college without letting me forget to stay calm and enjoy the best years of my life.

Abstract

This report examines the thermal degradation and corrosion of various amine solvents as they apply to amine scrubbing for CO_2 capture. Amines were placed in stainless steel cylinders and heated in convective ovens to simulate the stripping conditions inside a scrubbing unit. Samples were measured for remaining amine concentration, to test for degradation, and metals concentration, to estimate corrosion of the cylinder. The maximum stripping temperature of a particular compound, a measure of resistance to thermal degradation, strongly correlated with amine chain length. The linear amines studied had the following max temperatures: EDA (116 °C), PDA (124 °C), DAB (126 °C), BAE (130 °C), HMDA (140 °C), MEA (116 °C), MPA (129 °C), and DGA® (134 °C). The SHA/PZ blends had the following weighted max temperatures: AMP (143 °C), AMPD (135 °C), TRIS (130 °C), tBuAE (150 °C), PM (97 °C), and PE (129 °C). The linear amines follow initial first-order degradation curves, consistent with literature mechanisms. EDA, PDA, BAE, and AMP degraded significantly more slowly under acid conditions, suggesting that the degradation mechanisms do not incorporate CO_2. Acid loaded DAB degraded at a similar rate to CO_2-loaded conditions. MEA corroded 15 times faster than MPA; MAE corroded 3 times faster than EAE; DMAE-PZ corroded qualitatively faster than DMAP-PZ. These three pairs support the hypothesis that two-carbon chains corrode more than three-carbon chains. EDA corroded 40 to 80 times more than PDA according to older studies, seen in Figure 38, but more recent tests show similar corrosion rates where EDA is only 1.2 times faster (Figures 32 and 33). Corrosion and amine concentration correlate strongly; corrosion does not correlate strongly with temperature or CO_2-loading. Corrosion and formate generation appear to correlate, supporting corrosion mechanisms proposed in literature.

Table of Contents

List of Figures

List of Tables

Introduction

Amine Scrubbing

Global warming is one of the greatest environmental problems to face mankind. It is a scientific consensus that anthropogenic emissions of greenhouse gases, particularly CO_2, are the driving force behind recent increases in global temperatures. Efforts have been made to reduce CO_2 emissions from stationary sources, most importantly exhaust from fossil fuel combustion in power plants. Power plants make up 37% of US CO_2 emissions and the relatively high concentrations of CO_2 in their exhaust streams provide an easier target for carbon capture and storage (CCS) than air capture (European Parliament, 2013).

The leading CCS technology is amine scrubbing, a process in which basic amine solutions are contacted with a CO_2–rich stream in order to isolate the compound. An amine scrubbing unit includes an absorber and stripper column. The stream – flue gas from a stationary carbon source – flows into the absorber through the amine solvent. CO_2 absorbs into solution where it flows past a heat exchanger to the stripper. A reboiler heats the carbon-rich solvent to release the CO_2, which is then isolated and pressurized. The stripped solvent returns to the absorber and begins the process again. The decarbonized flue gas continues out the top of the absorber into the atmosphere. A diagram of this process is displayed in Figure 1 (CO_2CRC, 2013).
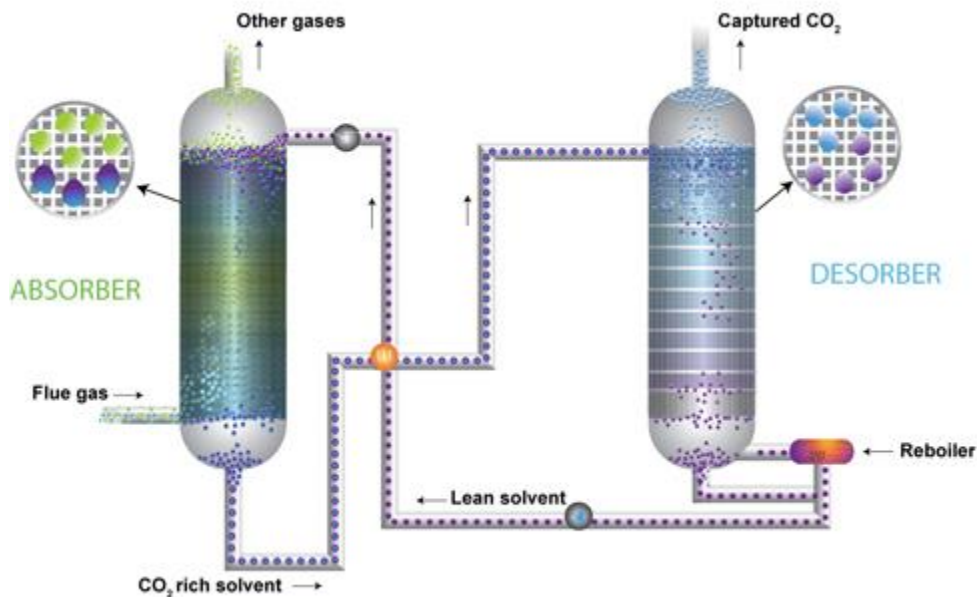
Fig. 1. Diagram of an amine scrubber. Flue gas enters the absorber on the left. Isolated CO_2 exits the desorber (stripper) on the right.

Flue gas enters the absorber with a CO_2 concentration ranging from 4 to 12%, depending on the combustion source. The scrubbing unit targets 90% decarbonisation of the inlet gas. Amine solvents are aqueous solutions containing 2.5 to 10 weigh percent amine, depending on the capacity of the compound to absorb CO_2 and the compound solubility. CO_2 loading in the solvent is defined as mol of CO_2 per mol of alkalinity, with alkalinity referring to an amino group capable of absorbing CO_2. The solvent will normally operate with lean and rich loadings of 0.15-0.3 and 0.3-0.45, respectively, as it cycles through the absorbing and stripping process. The absorber operates at atmospheric pressure and moderate temperature (40-70 ℃); the stripper operates at higher temperature and pressure (90-150 ℃, 2-20 bar), necessary conditions to reverse the CO_2 absorption reaction. Concentrated CO_2 leaves the stripper for compression to 150 bar. At this stage it can be transported to facilities for underground sequestration. There is limited use for purified CO_2; like H_2S sweetening, the primary motivation for CCS is to avoid environmental damage and associated fines. Purified CO_2 does see use in enhanced oil recovery, however. Although currently unprofitable under modern carbon regulations, amine scrubbing is expected to be economically feasible by 2035 (DOE, 2014).

There are several advantages to amine scrubbing over other proposed CCS technologies.

9

Scrubbing is a proven method that sees successful implementation in acid gas treating. The mechanics of scrubbing are well understood and can be readily modelled. Amine scrubbers can also be retrofitted to existing coal and gas fired power plants without significant modification in the design. An important disadvantage of amine scrubbing, however, is managing an inventory of amine. The process conditions lead to thermal degradation of the amine solvent and corrosion of the process metals.

Thermal Degradation

Thermal degradation refers to thermally induced side reactions that occur with the amine solution inside the stripper column. These reactions consume the original amine and produce unwanted side products. Thermal degradation is avoided by operating the stripper column at a sufficiently low temperature; however, the process is more efficient at higher stripper temperature, and there is motivation to identify the maximum acceptable temperature that each candidate solvent can be operated. High stripper temperatures also break down carcinogenic nitrosamines found in solution. Some studies in the literature discuss the mechanisms of diamine and alkanolamine degradation. Previous work suggests that MEA carbamate, the form the compound takes after reacting with and absorbing CO_2, degrades by a rate-limiting ring-closing reaction of the carbamate to form 2-oxazolidone (Davis, 2009):
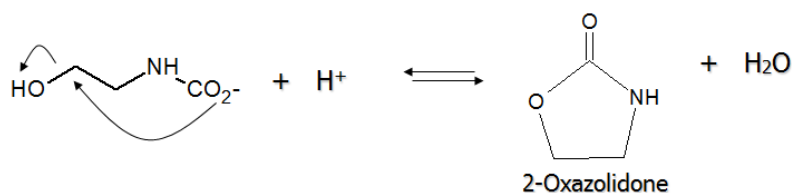
Fig. 2. MEA carbamate ring-closes to form 2-Oxazolidone

MEA can further react with 2-oxazolidone on the β-carbon to form oligomers in a process known as amine polymerization.

Work by Zhao (2010) predicts analogous rate-limiting steps for the degradation of EDA and PDA to form reasonably stable cyclic ureas:
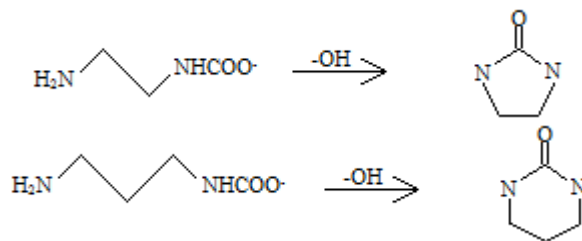
Fig. 3. EDA and PDA ring-close to form cyclic ureas.

MPA and PDA are expected to form similar cyclic products with stable six-membered rings. Larger molecules such as DAB are thought to eliminate the amino group and form a six-membered ring (Lepaumier, 2010):
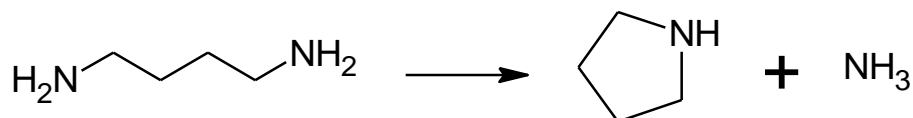
Fig. 4. Proposed degradation pathway of acidified DAB to form pyrrolidine. CO_2 serves as an acidifying catalyst and not a reactant.

Amines with complementing characteristics have been studied together in blends with some success. One notable example is solvents featuring sterically hindered amines (SHAs). A SHA is defined as a compound with an amino group that is sterically hindered by a branch on the alpha-carbon. These amines demonstrate good performance in conjunction with primary or secondary amines, especially with piperazine (PZ). SHA/PZ blends are interesting solvents because of their high capacity and fast rate of reaction with CO_2.

SHAs follow a different reaction pathway to absorb CO_2. An ordinary primary or secondary amine absorbs CO_2 by reacting to form a carbamate. This process requires two amino groups: one forms a N-C bond with the CO_2, and the other accepts a hydrogen and protonates. SHAs, on the other hand, are too hindered around the amino group to form stable carbamates. These compounds instead react with CO_2 to form a bicarbonate ion and a protonated amine. The former reaction is fast, but has a theoretical absorption limit of 0.5 mol CO_2/mol alkalinity because it requires two amino groups. The latter reaction is usually slow, but only occupies one amino group and therefore

has a higher capacity of 1 mol CO_2/mol alkalinity. A SHA/PZ blend takes advantage of both beneficial characteristics: the presence of PZ enables a fast absorption of CO_2, and the SHA increases overall solvent capacity.

Corrosion

Unlike thermal degradation, corrosion is much less studied in amine scrubbing literature. Work by Fischer argues that corrosion in the amine scrubber occurs by oxidizing metals and reducing CO_2 into formate (HCO_2^-), although this assertion is largely untested. The stripper environment is unique for most corrosion chemistry because the solution is largely oxygen-free and rich in CO_2; Fischer demonstrates this below in Figure 5 (Fischer, 2014).
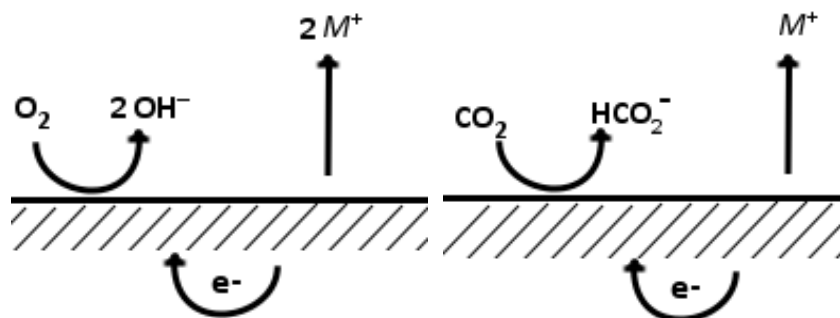
Fig. 5. Possible model of corrosion in an amine scrubber. Typical corrosion is shown on the left; low O_2/ high CO_2 corrosion is on the right.

One trend noticed in previous corrosion work is that amines with two-carbon chains separating functional groups appear to degrade far more than amines with three-carbon chains. Fischer attempts to explain this pattern with the following diagram:
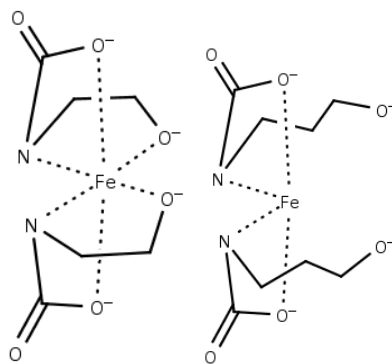
Fig. 6. MEA carbamate complexes more easily with iron ions than MPA carbamate.

Fischer argues that amine carbamates with two-carbon chains form relatively stable organometallic complexes with metal ions. Three-carbon chains, such as in MPA carbamate, are too long to complex with metals. This report aims to test this hypothesis by comparing the corrosion of several two/three carbon analogues.

The purpose of this report is to determine a relationship between thermal degradation, corrosion, and amine structure. It is necessary to understand the mechanisms behind these two types of reactions in order to make informed decisions about process design. The correct choice of scrubbing solvent will make the amine scrubbing more environmentally friendly and more efficient in the long run.

Experimental Methods

Amine solutions were prepared to a specific concentration and CO_2 loading to simulate process conditions. The specified concentration was generally 10 molal alkalinity, with alkalinity referring to a primary or secondary amino group capable of absorbing CO_2. All monoamine solutions were 10 molal and all diamine solutions were 5 molal, with an exception for HMDA, which was prepared at 2.5 molal to remain soluble.

Solutions were loaded with CO_2 by sparging the dilute amine in a glass cylinder. CO_2 loading is measured as a ratio of mol of CO_2 in solution to mol of alkalinity in solution, represented by the symbol α. Loadings for the degradation and corrosion experiments range from $\alpha = 0.2$ to $\alpha = 0.45$, with the former matching the process lean loading and the latter nearing the theoretical limit for CO_2 loading. Typical process conditions use a rich loading of $\alpha = 0.35$ in the stripper.

Gravimetrically prepared solutions were placed inside Swagelok® 316L stainless steel cylinders. Each cylinder had a volume of 4.5 ml (10 cm long, 3/8 in. ID) and was rated to 130 barg. Cylinders were heated in convective ovens for 24 to 1000 hours, depending on the requirements of the particular experimental series. Cylinders containing samples not analysed for corrosion were periodically removed from the oven and stored in a freezer to halt degradation. When the series finished, all cylinders were simultaneously opened, stored in glass vials, and analysed. Cylinders involved in corrosion studies were immediately quenched and emptied into glass vials once removed from the oven. This precaution was taken to prevent additional corrosion in the freezer, waiting for the experimental series to complete.
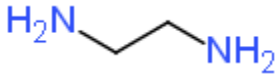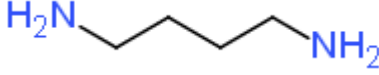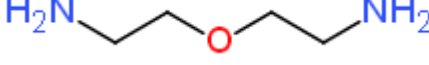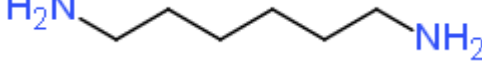
Amine degradation was measured using cation chromatography. A Dionex® ICS-2100 chromatograph analysed samples for relative concentration of the parent amine. Samples were diluted 10000x with distilled, deionized water (DDI) before being analysed by the chromatograph. Samples were run through a 4 mm x 250 mm CS17 analytic column. Comparison with a prepared standard yielded absolute concentrations of the amine in each sample. Different species eluted from the system at different times, allowing for discrimination between the parent amine and degradation by-products. The methods of analysis and preparation of degradation studies reported
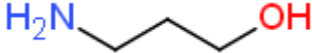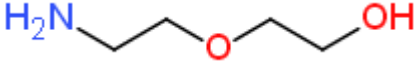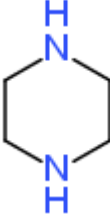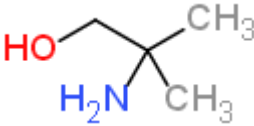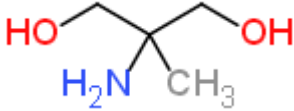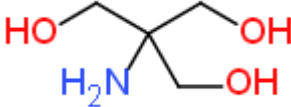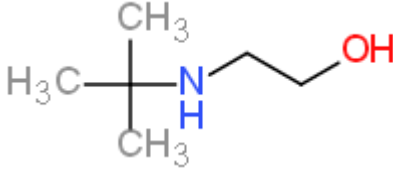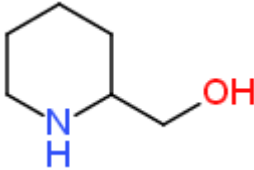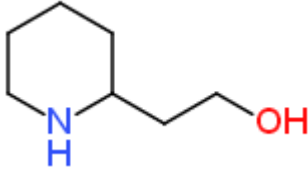
in this report are similar to Namjoshi (2015) and Freeman (2011).

Dissolved metals were measured with assistance of Kent Fischer with inductively coupled plasma optical emission spectroscopy (ICP-OES). Analysis was performed using an axial-configured Varian 710-ES unit. Samples were diluted 30x with a 2 wt% HNO_3 solution before being run. The unit measured for concentrations of chromium, iron, manganese, molybdenum, and nickel, each calibrated to a 1000 ppm Fischer Chemicals reference standard.
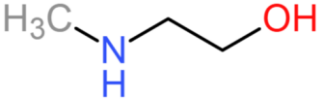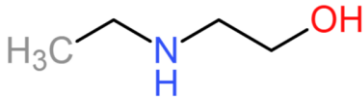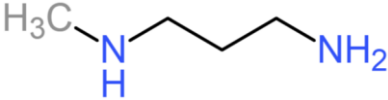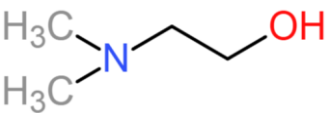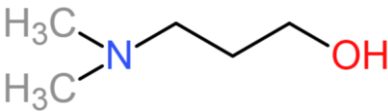
Degradation and corrosion data of several alkanolamines, diamines, and SHAs is presented in this report. Table 1 lists the abbreviation, formal name, and molecular structure of each amine.

Table 1: List of Amines

Name	Structure
EDA 1,2-diaminoethane	
PDA propane-1,3-diamine	
DAB butane-1,4-diamine / putrescine	
BAE 2-(2-aminoethoxy)ethanamine	
HMDA hexane-1,6-diamine	
MEA 2-aminoethanol	

MPA 3-aminopropanol	
DGA® 2-(2-aminoethoxy)ethanol	
PZ piperazine	
AMP 1-amino-2-methyl-1-propanol	
AMPD 2-amino-2-methyl-1,3-propanediol	
TRIS 2-amino-2-(hydroxymethyl)-1,3-propanediol	
tBuAE 2-(*tert*-butylamino)ethanol	
PM 2-piperadinemethanol	
PE 2-piperadineethanol	

MAE 2-methylaminoethanol	H₃C—NH—CH₂CH₂—OH *(structure: H3C–N(H)–CH2–CH2–OH)*
EAE 2-(ethylamino)ethanol	*(structure: H3C–CH2–N(H)–CH2–CH2–OH)*
MAPA 3-(methylamino)propylamine	*(structure: H3C–N(H)–CH2–CH2–CH2–NH2)*
DMAE 2-(dimethylamino)ethanol	*(structure: (H3C)2N–CH2–CH2–OH)*
DMAP 3-(dimethylamino)propanol	*(structure: (H3C)2N–CH2–CH2–CH2–OH)*

Because the purpose of this experiment is to find a degradation-structure relationship, many of the examined amines have similar functional groups and only vary by one feature. The diamines, for example, increase in chain length from EDA (2 carbon chain) to HMDA (6 carbon chain). Each alkanolamine is an analogue to a selected diamine. SHA blends of AMP, AMPD, and TRIS with PZ vary by replacing one methyl group with a hydroxyl group. The final five entries in the list – MAE, EAE, DMAE, DMAP, and MAPA – were only tested for corrosion, not degradation.

Results

Thermal Degradation

Figures 7 through 9 show the degradation of EDA, PDA, DAB, BAE, and HMDA, the five diamines investigated in this report. Each diamine was degraded as a 5 m amine solution with CO_2 α = 0.4. HMDA was an exception, requiring a lower concentration of 2.5 m to remain soluble in water. Amines were degraded at 165 ºC, 150 ºC, and 135 ºC.
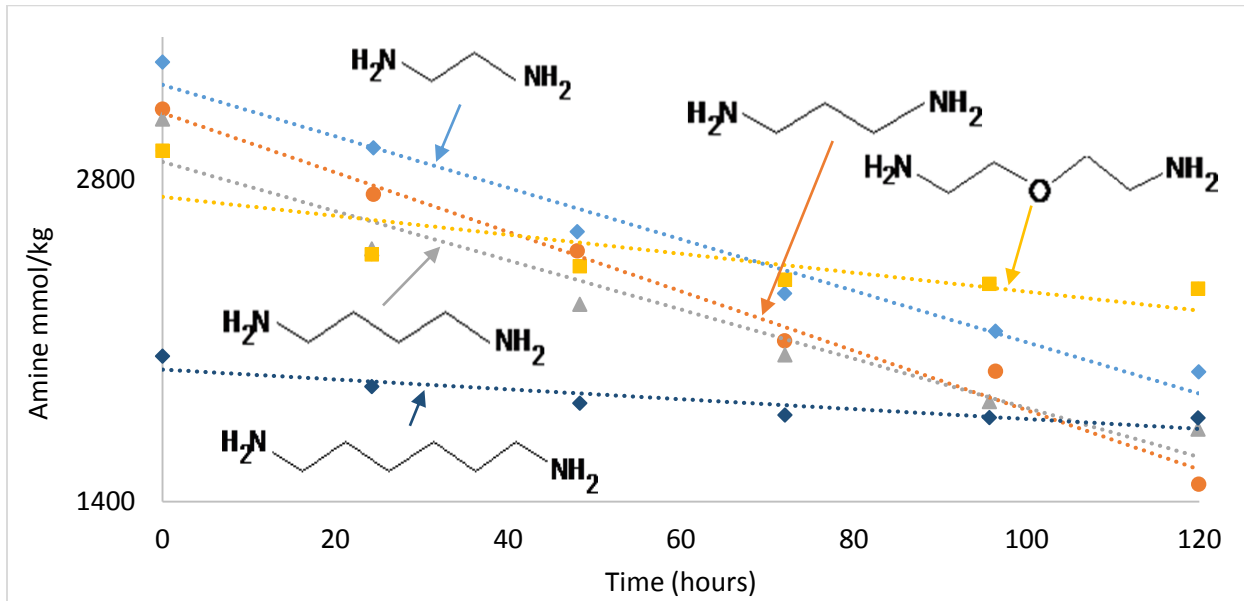
Fig. 7. 5 m EDA, 5 m PDA, 5 m DAB, 5 m BAE, and 2.5 m HMDA degraded at 165 °C and 0.4 CO_2 loading. BAE appears to reach equilibrium with the degradation products.
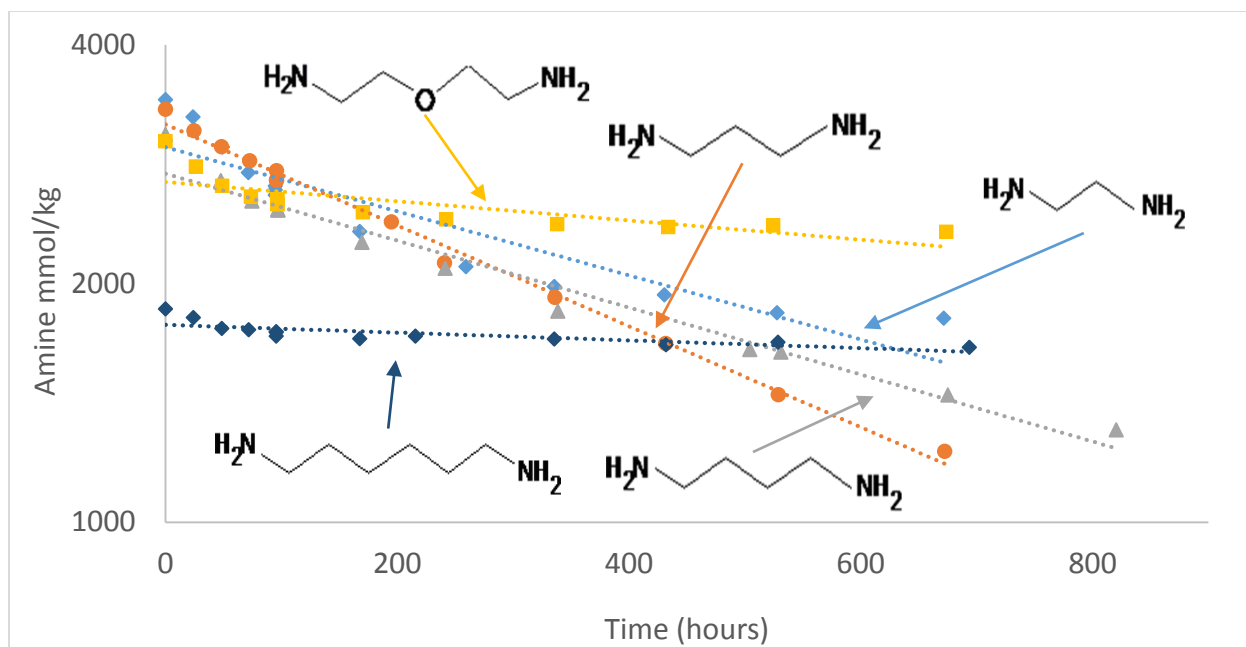
Fig. 8. 5 m EDA, 5 m PDA, 5 m DAB, 5 m BAE, and 2.5 m HMDA degraded at 150 °C and 0.4 CO_2 loading. EDA, BAE, and HMDA appear to reach equilibrium with the degradation products.
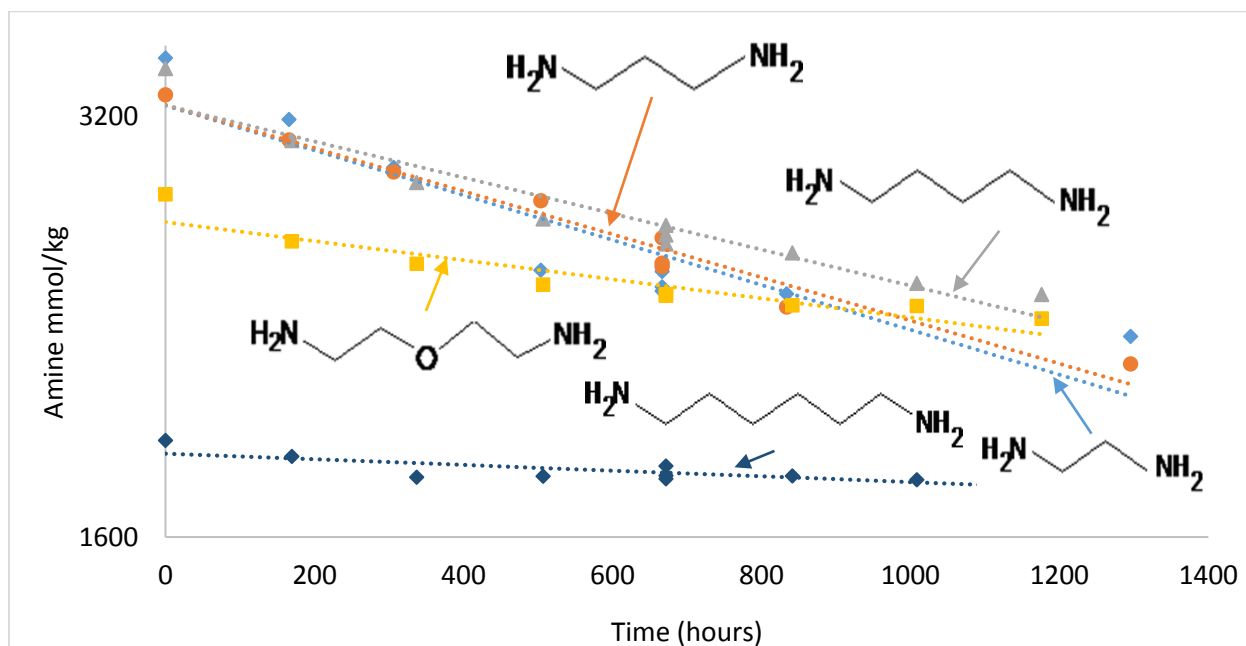
Fig. 9. 5 m EDA, 5 m PDA, 5 m DAB, 5 m BAE, and 2.5 m HMDA degraded at 135 °C and 0.4 CO_2 loading. EDA, BAE, and HMDA appear to reach equilibrium with the degradation products.

The concentration axis in each plot is a base-2 log scale. A linear fit in this scale represents exponential decrease in concentration, indicative of first-order degradation mechanisms. PDA and DAB follow strong first-order trends. EDA, BAE, and HMDA appear follow an initial first-order degradation before levelling off. These compounds likely reach equilibrium with their degradation products, a phenomenon expected in batch reactors.

Figures 10 through 12 display similar degradation plots for the three alkanolamines examined (MEA, MPA, and DGA®). MEA and MPA were degraded at 10 m amine concentration; DGA®, due to solubility issues, was degraded at 5 m concentration. Having only one amino group, the concentrations of these alkanolamines represent the same concentration of alkalinity as their diamine analogues. Each alkanolamine was loaded to CO_2 α = 0.4 and was degraded at 165 ℃, 150 ℃, and 135 ℃.
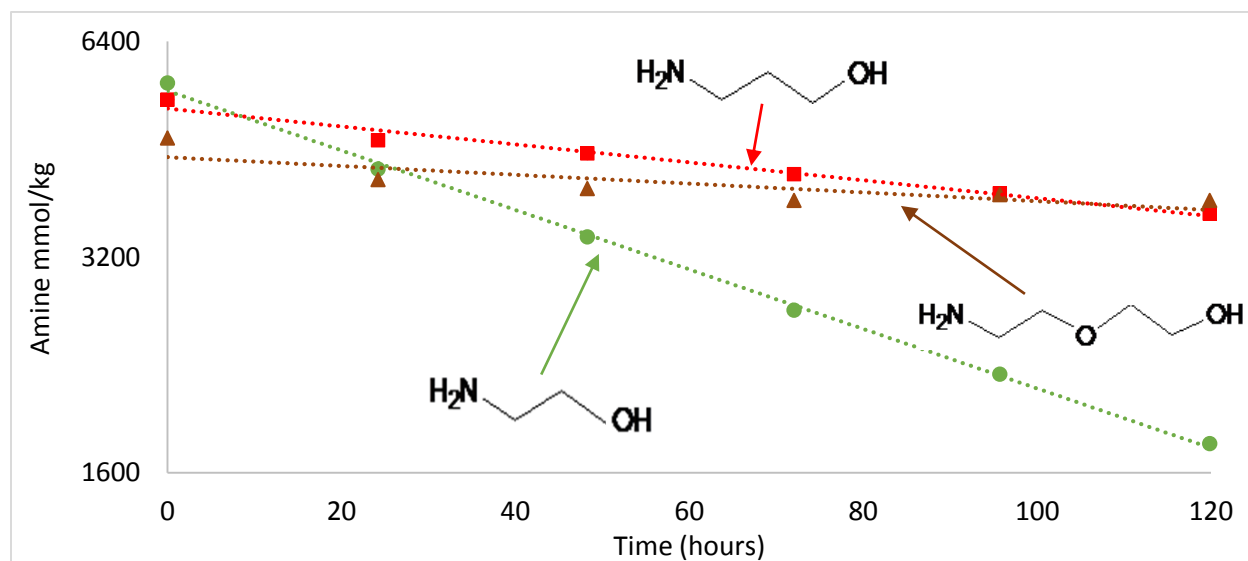
Fig. 10. 10 m MEA, 10 m MPA, and 5 m DGA® degraded at 165 °C at 0.4 CO_2 loading. DGA® appears to reach equilibrium with the degradation products.
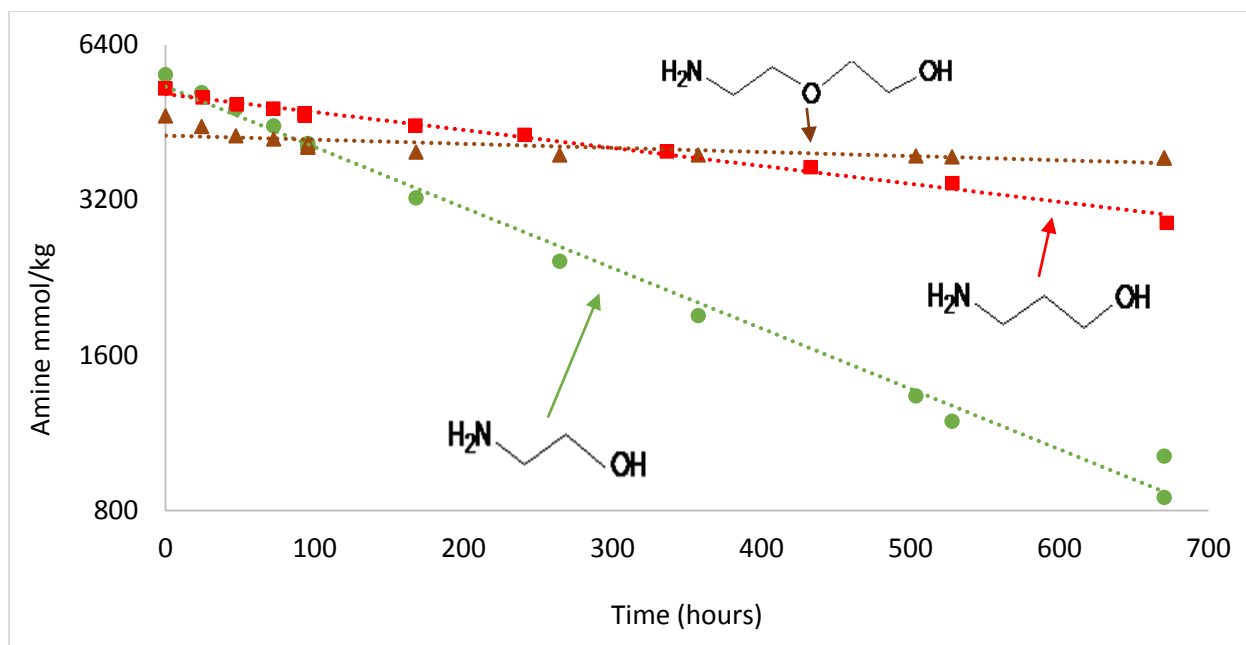
Fig. 11. 10 m MEA, 10 m MPA, and 5 m DGA® degraded at 150 °C at 0.4 CO_2 loading. DGA® appears to reach equilibrium with the degradation products.
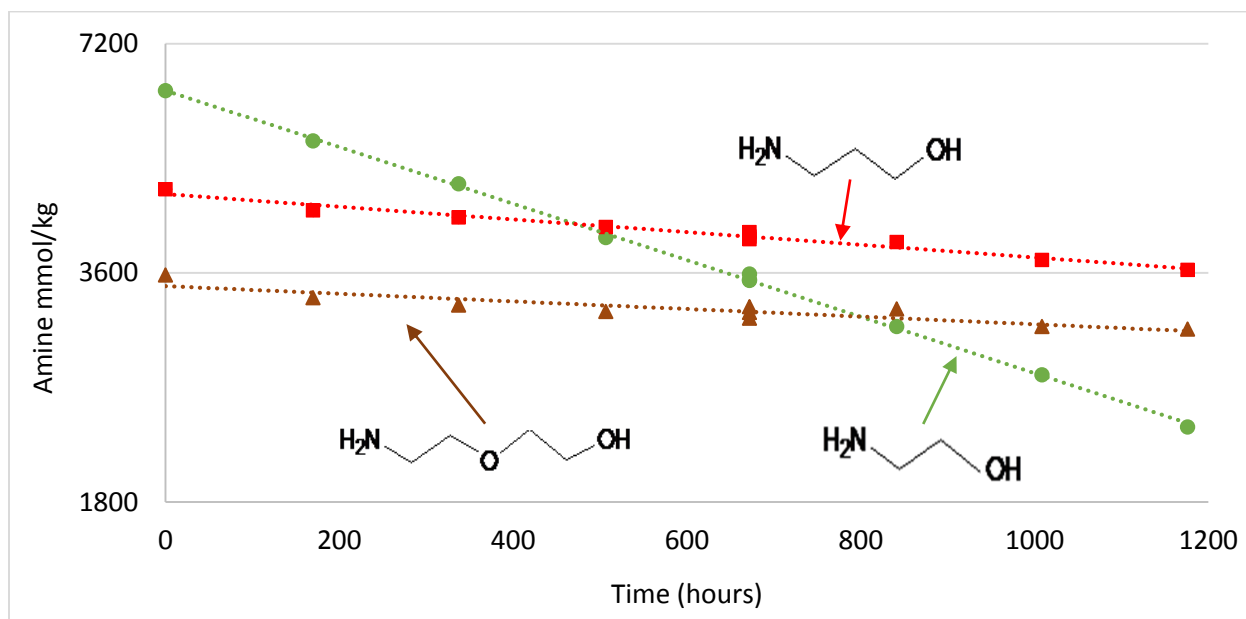
Fig. 12. 10 m MEA, 10 m MPA, and 5 m DGA® degraded at 135 °C at 0.4 CO_2 loading. DGA® appears to reach equilibrium with the degradation products.

Concentrations are again plotted on a base-2 log scale. MEA and MPA consistently demonstrate first-order degradation behaviour, while DGA® appears to reach equilibrium with the degradation products.

Table 2 lists first-order rate constants (units of hr^{-1}) taken from each diamine and alkanolamine across the three temperatures. The rate constants of EDA, BAE, HMDA, and DGA® were calculated only from the initial, linear regions of the concentration plot.

Table 2. First-order rate constants (hr^{-1}) for degradation reactions and associated activation energies (kJ/mol). The "eq" subscript indicates that the amine reached equilibrium with its degradation products. Amines are ordered by degradation rate at 165 °C.

Amine	165 °C $CO_2 = 0.4$ (hr^{-1}*e5)	165 °C Acid = 0.2 (hr^{-1}*e5)	150 °C $CO_2 = 0.4$ (hr^{-1}*e5)	135 °C $CO_2 = 0.4$ (hr^{-1}*e5)	Activation Energy (kJ/mol)	Maximum Temperature (°C)
10 m MEA	956	n/a	270	86	120	116
5 m PDA	639	69	147	36	140	124
5 m EDA	553	142	287^{eq}	56 ^{eq}	110	116
5 m DAB	529	457	97	30	140	126
5 m BAE	515^{eq}	16	105^{eq}	22 ^{eq}	160	130
10 m MPA	288	n/a	80	19	130	129
5 m DGA®	262^{eq}	n/a	131^{eq}	14 ^{eq}	150	134
2.5 m HMDA	173	n/a	69^{eq}	7 ^{eq}	160	140

Fitting all three rate constants to a temperature dependent Arrhenius equation yields an activation energy of degradation. This value is used to calculate the maximum acceptable temperature of operation for each amine. Maximum temperature is defined as the temperature that induces a two-percent loss per week of amine to thermal degradation. The value appears to correlate very strongly with amine chain length; for both diamines and alkanolamines, increasing the chain length always increases the max temperature.

Also included in Table 2 are degradation rate constants of acid-loaded amines. Figure 13 below

displays the degradation of EDA, PDA, DAB, and BAE at 165 ºC under acidified conditions of 0.2 mol H^+/mol alkalinity and 5 m amine concentration.
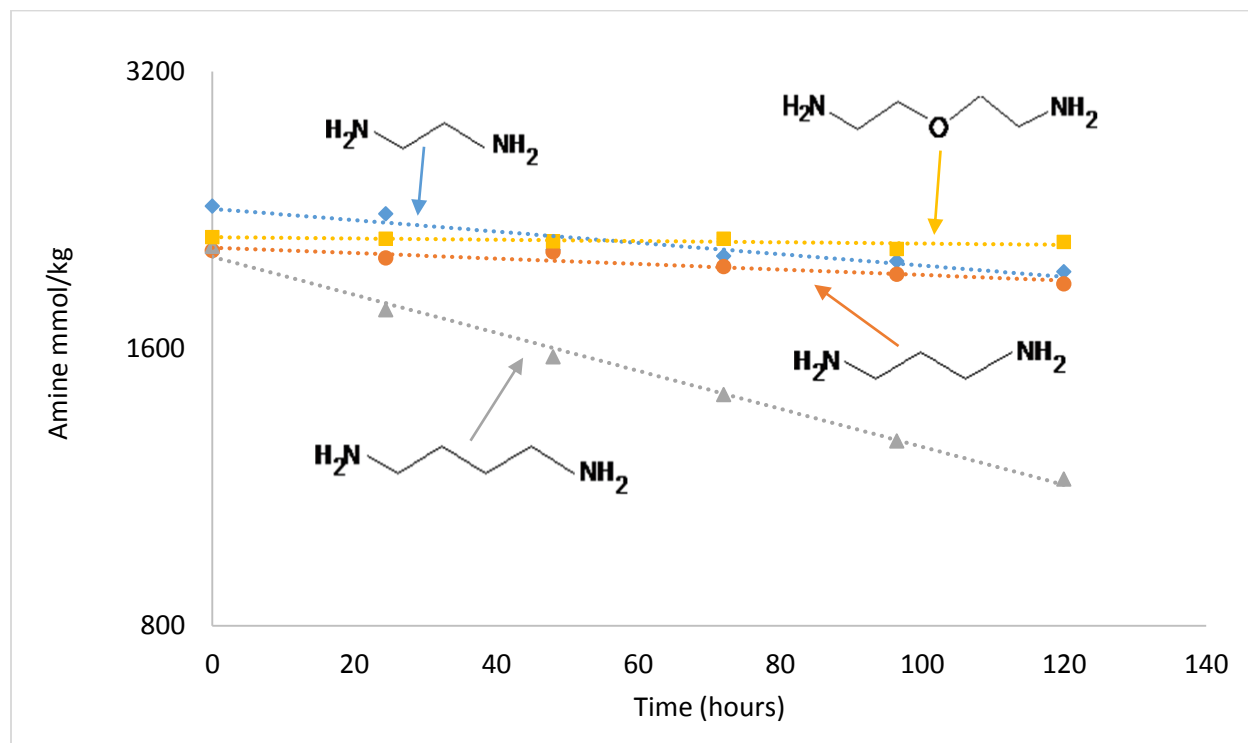
Fig. 13. EDA, PDA, DAB, and BAE degraded at 165 °C at 0.2 H^+ loading and 5 m concentration. DAB maintains a similar degradation rate in acid conditions but the other three amines slow down significantly.

EDA, PDA, and BAE all degrade much more slowly under acidified conditions. The rate constants are tabulated in Table 2. The rate constant for EDA drops from .00553* hr^{-1} to 0.00142 hr^{-1}, for PDA from 0.00639 hr^{-1} to 0.00069 hr^{-1}, and for BAE from 0.00515 hr^{-1} to 0.00016 hr^{-1}. The degradation rate constant of DAB drops much less, from 0.00529 hr^{-1} to 0.00457 hr^{-1}. This small change compared to the other three amines suggests that DAB degrades by some mechanism that does not incorporate CO_2 into the final degradation product. This would be consistent with the reaction proposed in Figure 4.

This mechanism involves the protonation of an amino group and subsequent attack on the alpha carbon by the other, non-protonated amino group of the DAB molecule. The molecule ring-closes

to form pyrrolidine and eliminates an ammonia molecule. EDA and PDA do not appear to degrade as significantly under acid loading, and more likely follow reactions that combine with CO_2 to form a cyclic urea, as in Figure 2. BAE hardly degrades at all under acid loading but has too long a chain to form a cyclic urea by the above mechanism.

Figures 14 through 19 plot the degradation of five of the six SHA/PZ blends. PM/PZ degrades so rapidly that the concentrations cannot be easily compared with the other blends in the same graph; the degradation of PM/PZ is plotted in figures 20 and 21.
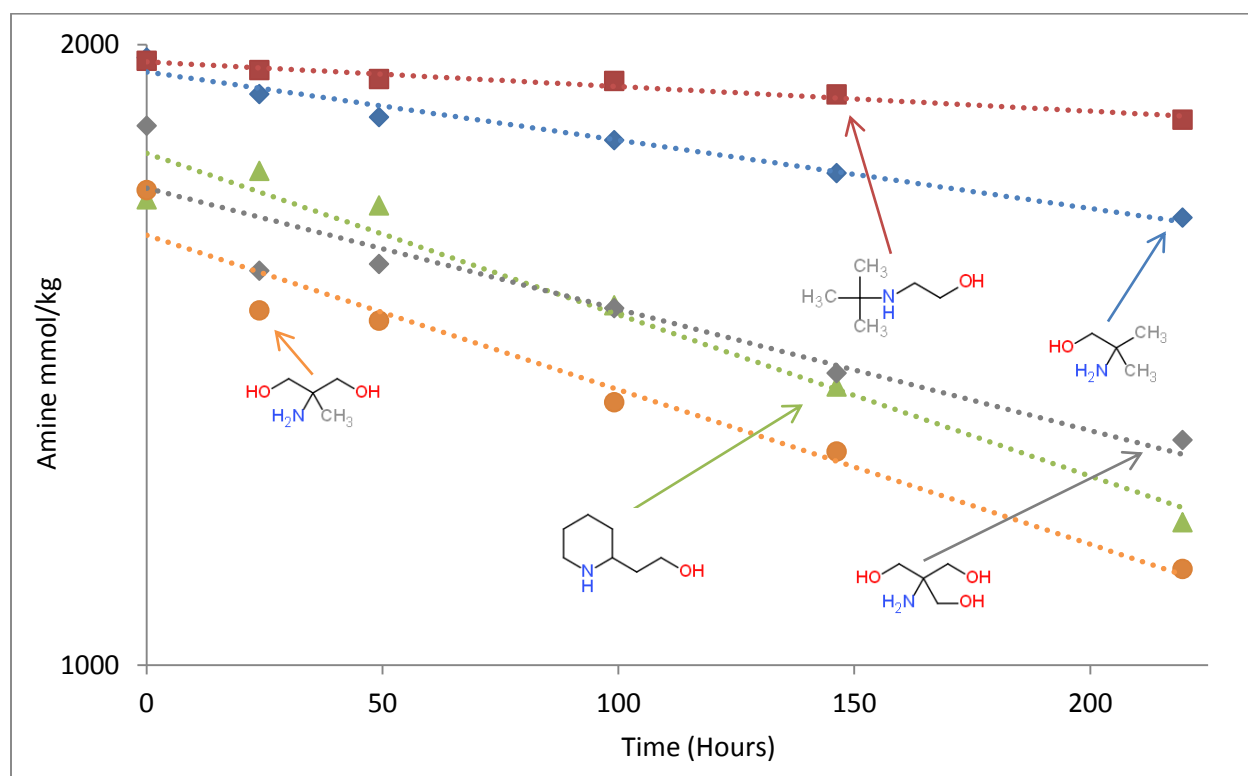
Fig. 14. SHAs in 2.67 m SHA/1.33 m PZ degraded at 165 ºC and CO_2 α = 0.22.
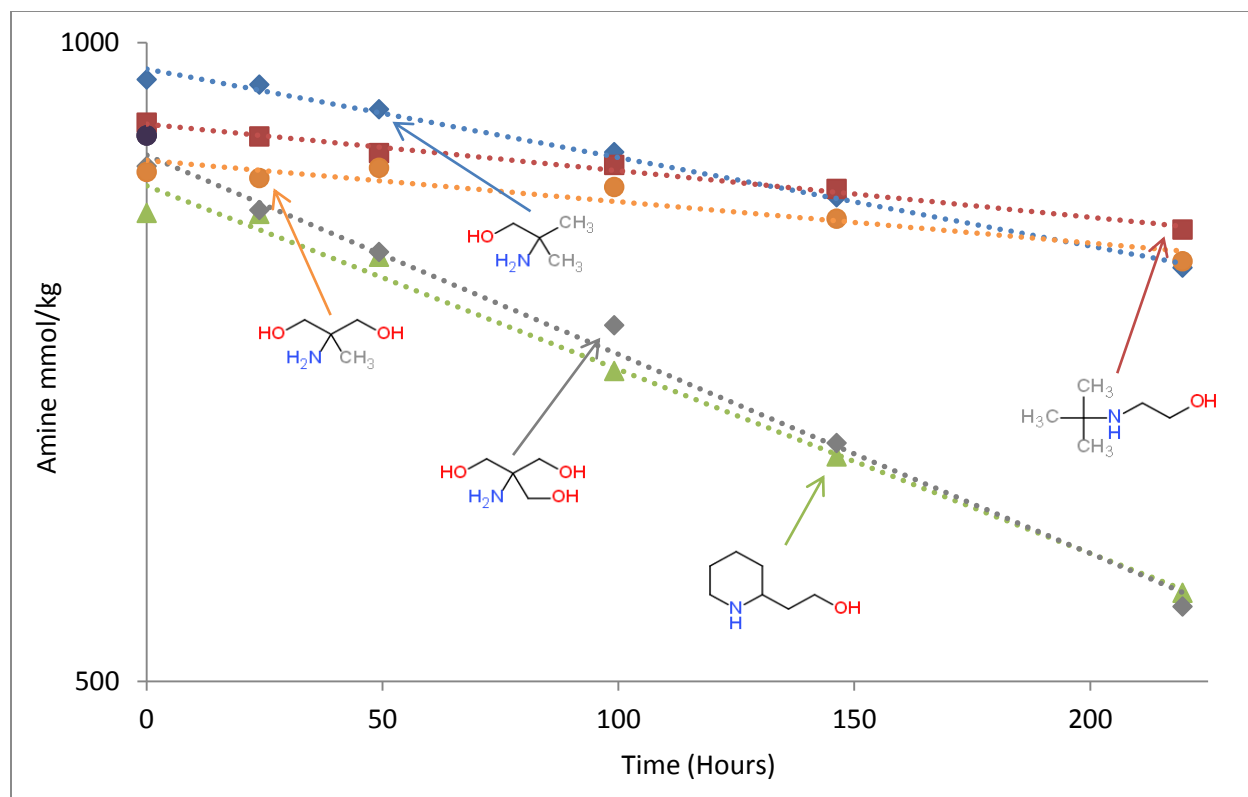
Fig. 15. PZ in 2.67 m SHA/1.33 m PZ degraded at 165 ºC and CO_2 α = 0.22.
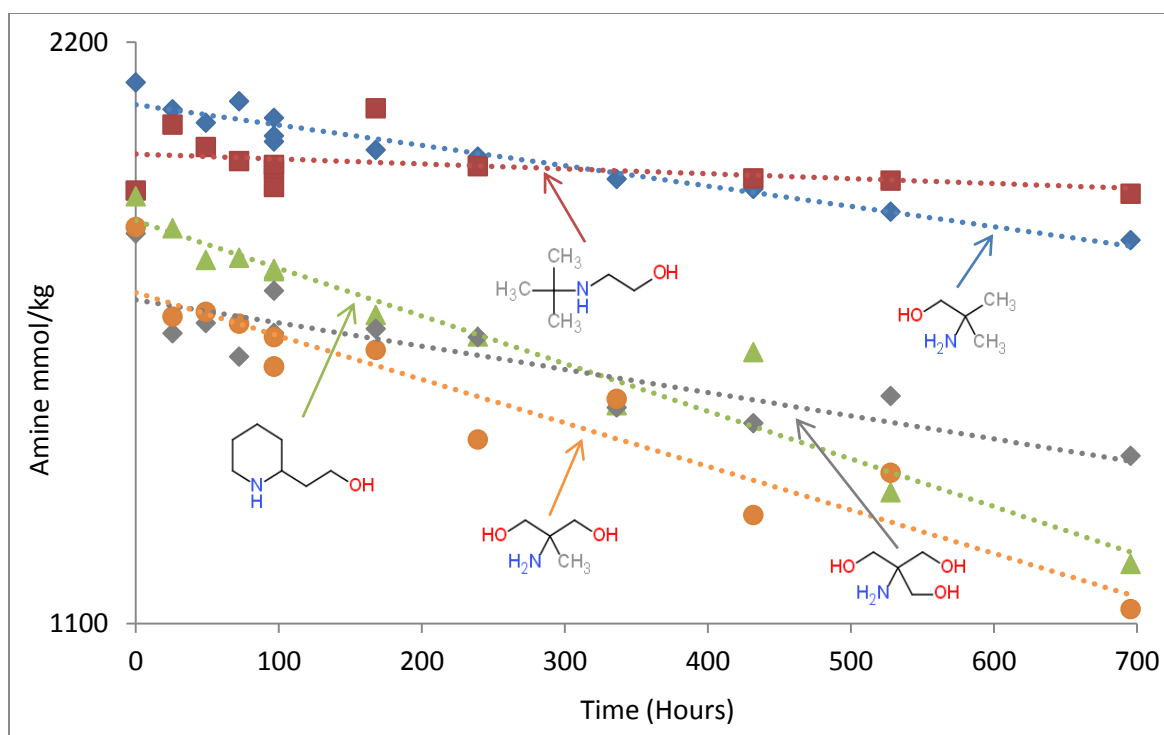
Fig. 16. SHAs in 2.67 m SHA/1.33 m PZ degraded at 150 ºC and CO_2 α = 0.22.
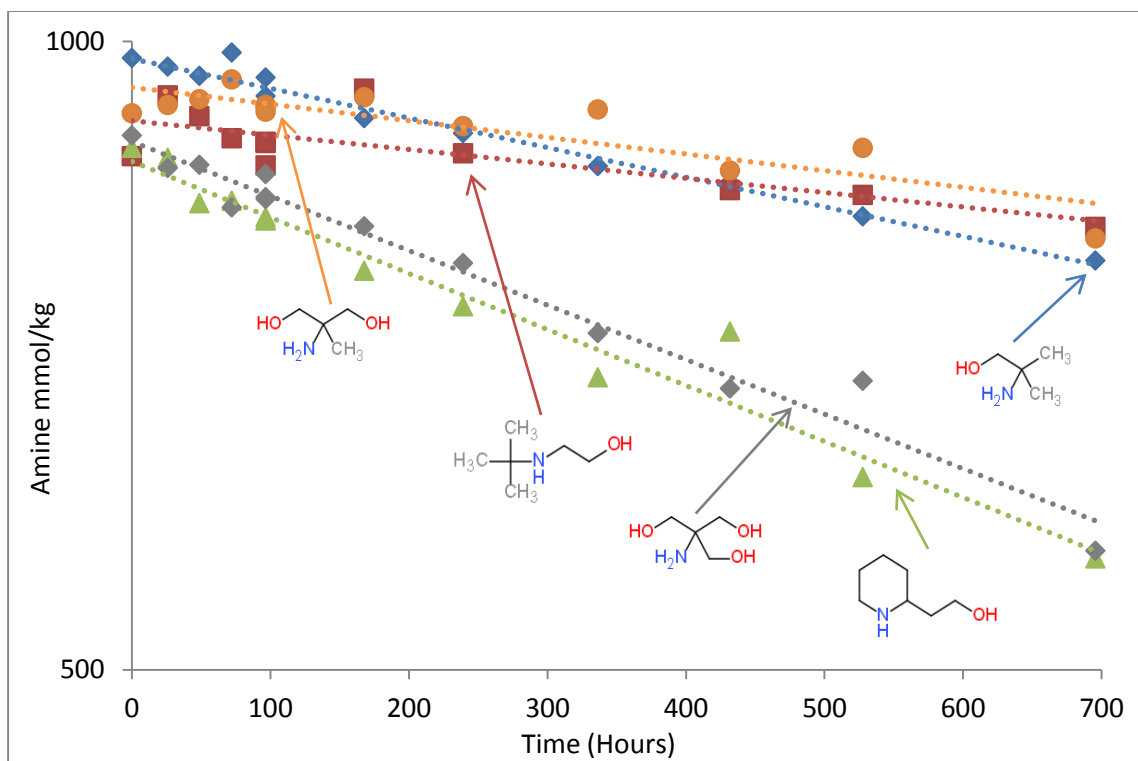
Fig. 17. PZ in 2.67 m SHA/1.33 m PZ degraded at 150 ºC and CO_2 $\alpha = 0.22$.
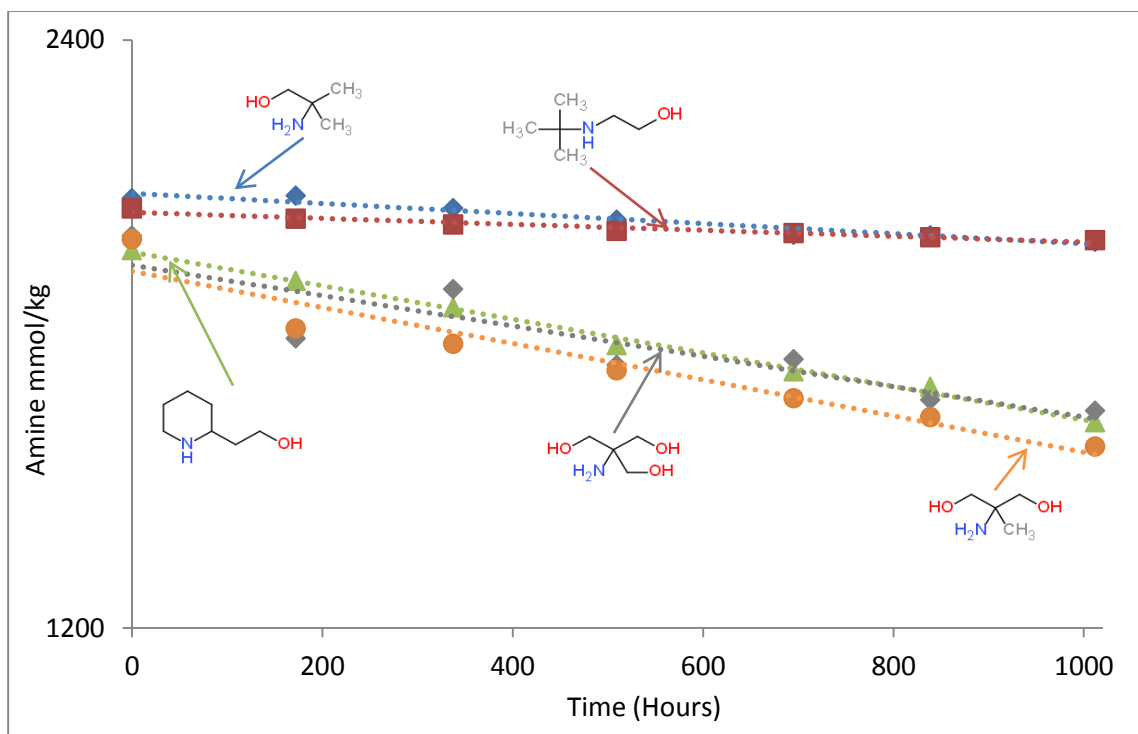
Fig. 18. SHAs in 2.67 m SHA/1.33 m PZ degraded at 135 ℃ and CO$_2$ α = 0.22.
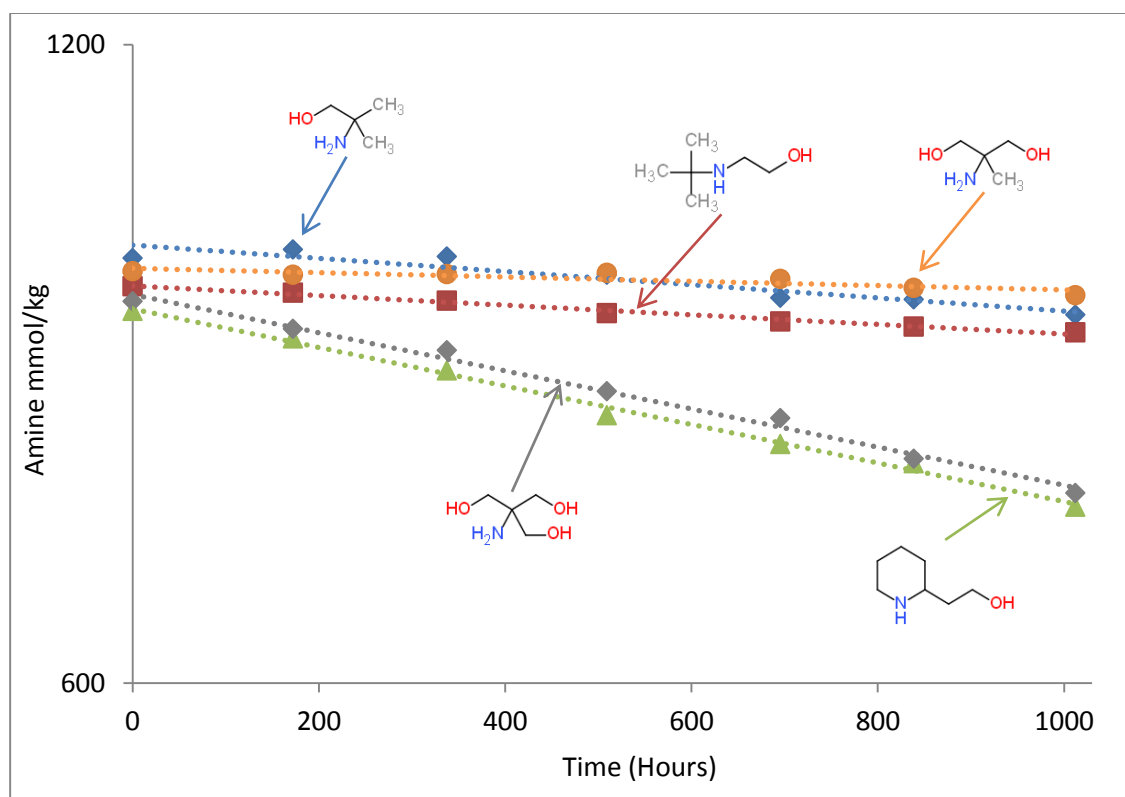
Fig. 19. PZ in 2.67 m SHA/1.33 m PZ degraded at 135 ℃ and CO$_2$ α = 0.22.
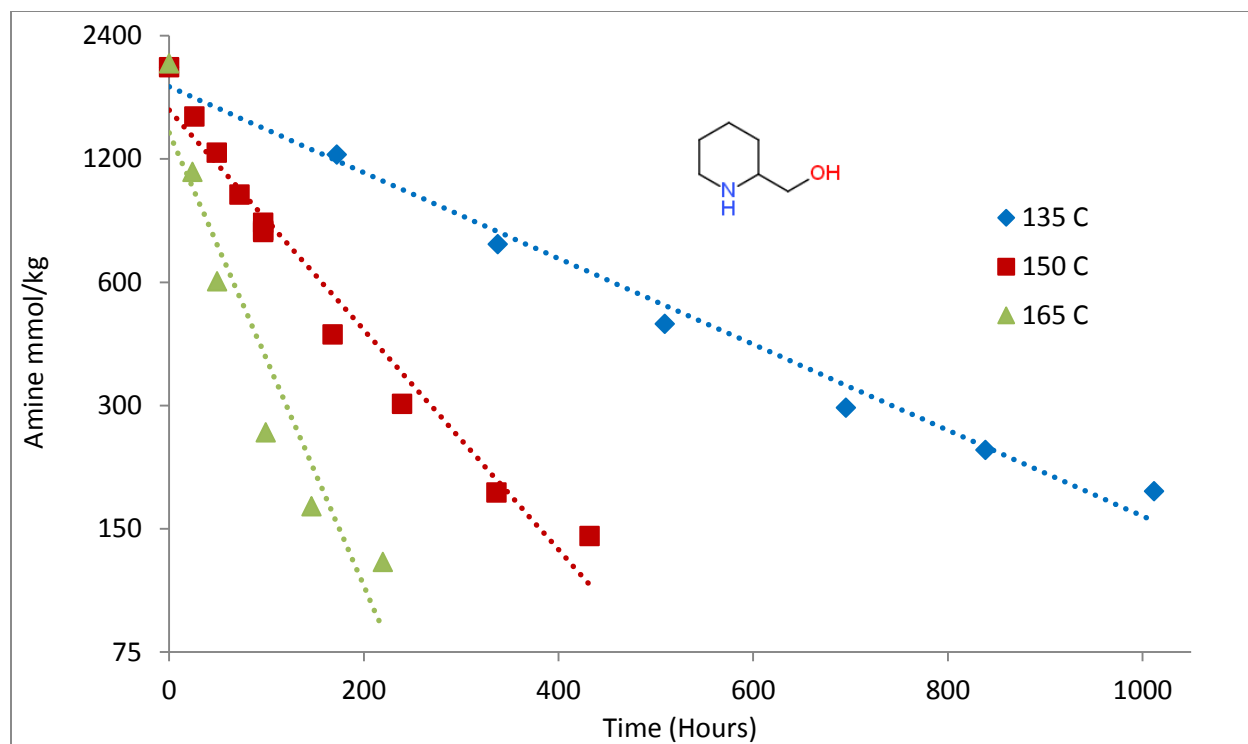
Fig. 20. PM in 2.67 m PM/1.33 m PZ degraded at CO_2 α = 0.22 and variable temperature.
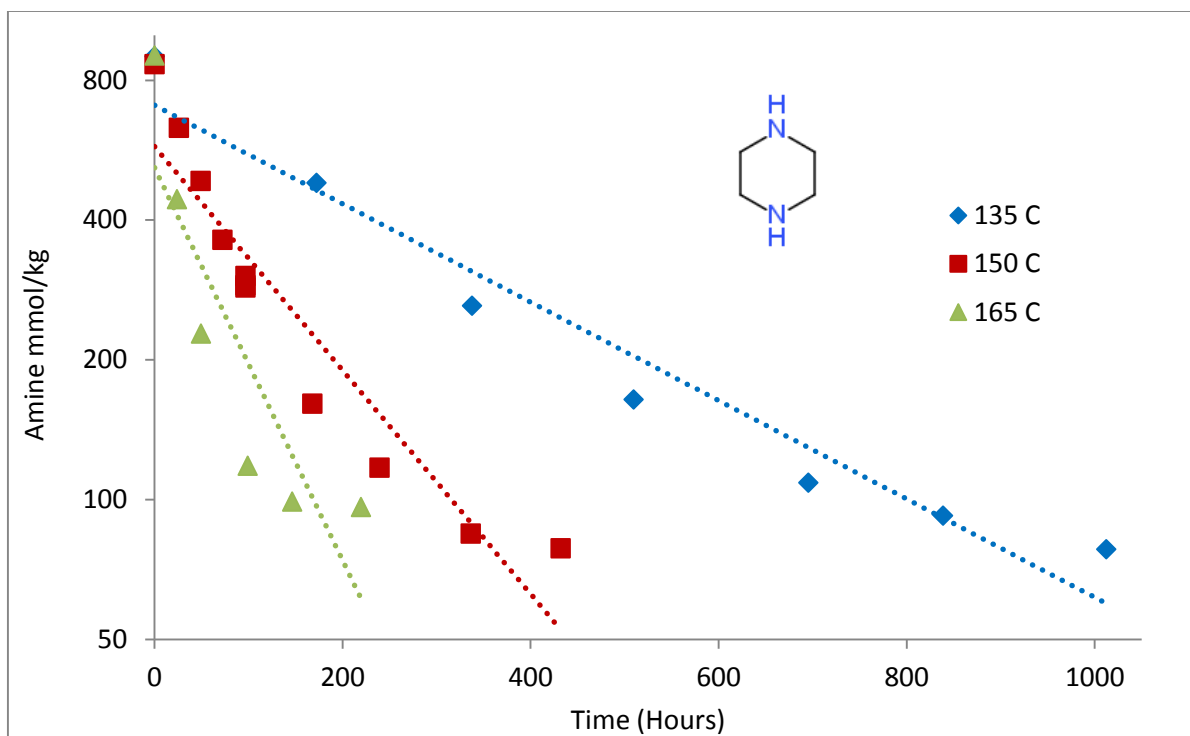
Fig. 21. PZ in 2.67 m SHA/1.33 m PZ degraded at CO_2 α = 0.22 and variable temperature.

The degradation plots are linear on a log scale, indicative of first-order rate kinetics. The exception is degradation in PM/PZ, which demonstrates first-order kinetics at higher concentrations but appears to significantly slow over time. This behaviour suggests that PM/PZ is reaching chemical equilibrium with the degradation products.

The amines sort themselves into three distinct levels of stability. The least stable solvent is PM/PZ, the moderately stable solvents are PE/PZ and TRIS/PZ, and the most stable solvents are AMP/PZ and tBuAE/PZ. AMPD/PZ behaves differently; while AMPD degrades at rates similar to the moderately stable amines PE/PZ and TRIS/PZ, the PZ degrades at rates similar to the most stable amines AMP/PZ and tBuAE/PZ. Rate constants of these degradation plots are listed below in Table 2.

Figures 22 and 23 demonstrate the effect of concentration on AMP/PZ degradation. The first plot compares the degradation of AMP in 2.67 m AMP/1.33 m PZ, taken from the figures above, with that of AMP in a 4 m AMP/2 m PZ, keeping CO_2-loading constant. The second plot demonstrates the same effect of concentration on PZ degradation.
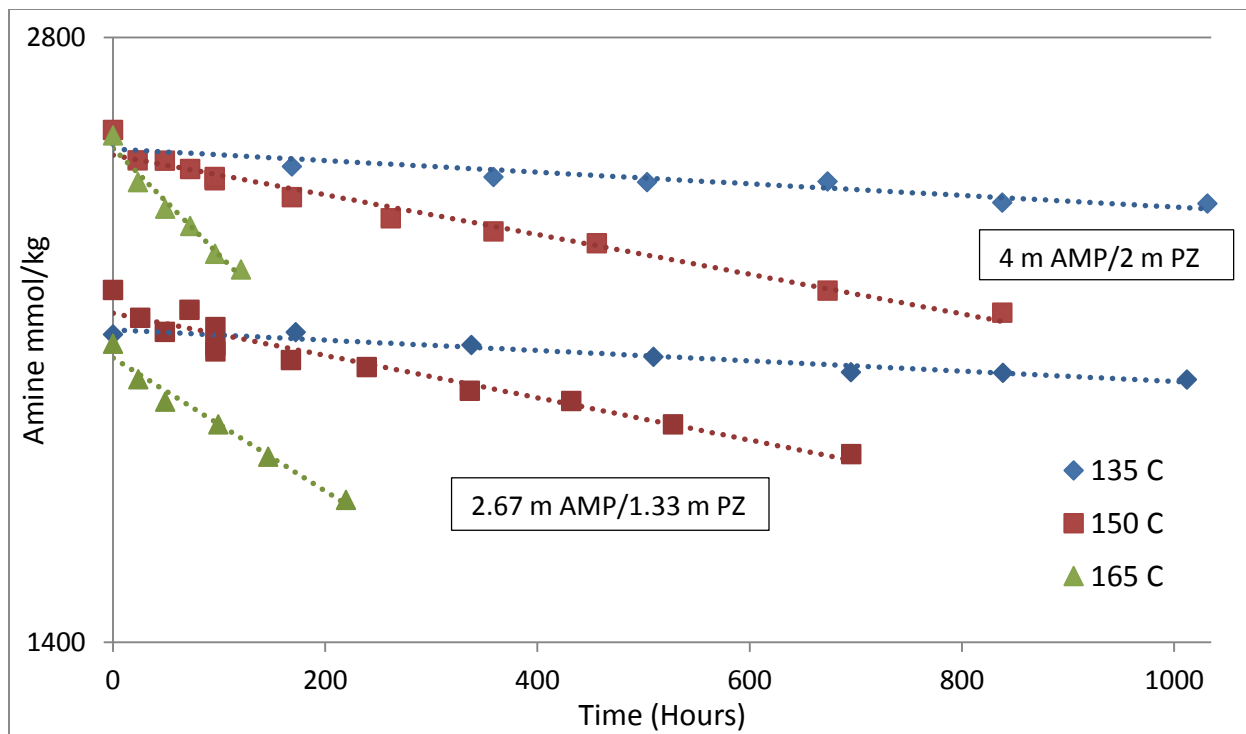
Fig. 22. Degradation of AMP in AMP/PZ at variable temperature and concentration and CO2 α = 0.22. 4 m AMP/2 m PZ is at the top of plot; 2.67 m AMP/1.33 m PZ is at the bottom.
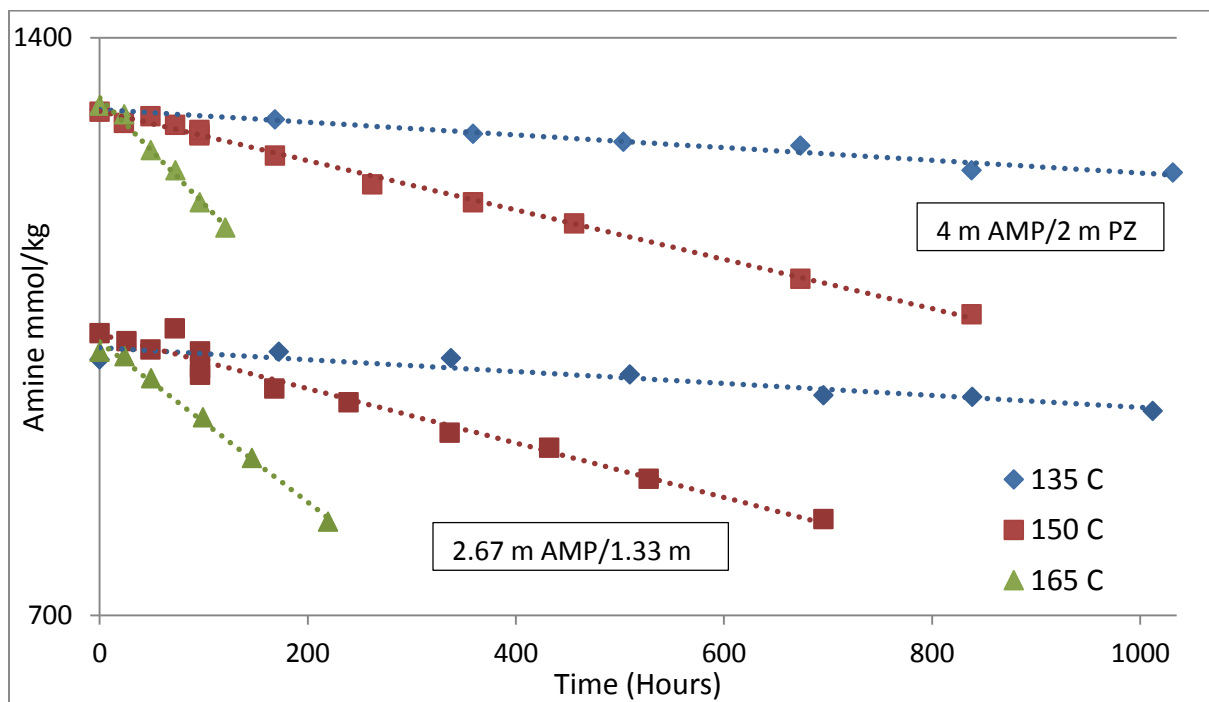
Fig. 23. Degradation of PZ inn AMP/PZ at variable temperature and concentration and CO_2 α = 0.22. 4 m AMP/2 m PZ is at the top of plot; 2.67 m AMP/1.33 m PZ is at the bottom.

AMP in the 2.67 m blend and 4 m blend degrades with a reaction rate of 5.9e-5 hr^{-1} and 6.7e-5 hr^{-1}, respectively, at 135 ºC; 2.42e-4 hr^{-1} and 2.27e-4 hr^{-1} at 150 ºC; and 7.63e-4 hr^{-1} and 1.224e-3 hr^{-1} at 165 ºC. PZ degrades with reaction rates of 7.2e-5 hr^{-1} and 7.6e-5 hr^{-1} for the 2.67 m and 4 m blend at 135 ºC; 3.26e-4 hr^{-1} and 2.96e-4 hr^{-1} at 150 ºC; and 9.61e-4 hr^{-1} and 1.272e-3 hr^{-1} at 165 ºC. Reaction rates at 135 ºC and 150 ºC are very similar across both concentrations for both species; reaction rates at 165 ºC appear to be higher for 4 m AMP/2 m PZ.

Table 3 lists the reaction rates in hr^{-1} of both species in all six blends at the three different temperatures studied, as well as reaction rates of species in the 4 m AMP/2 m PZ blend, taken from the previous eight figures.

Table 3: List of reaction rates in hr^{-1} and activation energies in kJ/mol. Rates and activation energies are presented for the SHA (at the top of the table) and for PZ (at the bottom of the table, in bold) for each blend at 135 ºC, 150 ºC and 165 ºC. CO$_2$ α = 0.22. Unless otherwise specified, concentrations are in 2.67 m SHA/1.33 m PZ. Because max temperatures are weighted 2:1 between the amine and PZ, only one set of values is presented.

Amine	135 ºC (hr^{-1}*e5)	150 ºC (hr^{-1}*e5)	165 ºC (hr^{-1}*e5)	Activation Energy (kJ/mol)	Maximum Temperature (°C)
AMP	5.9	24.2	76.3	130	143
4 m AMP	6.7	22.7	122.4	140	140
AMPD	21.3	51.8	172.7	100	135
TRIS	17.9	27.7	135.4	100	130
PM	294.4	926.3	2486.5	110	150
PE	21.3	56.8	180.2	110	97
tBuAE	3.5	5.8	27.5	100	129
AMP	7.2	32.6	96.1	130	n/a
4m AMP	7.6	29.6	127.2	140	n/a
AMPD	2.3	18.4	44.9	150	n/a
TRIS	20.7	60.1	216	120	n/a

PM	366.2	1115.6	2795.1	100	n/a
PE	20.9	61.8	199.4	110	n/a
tBuAE	5.2	15.8	50.5	110	n/a

The max temperature of a blend is defined differently than that of single amines. The value presented in Table 3 is a 2 to 1 weighted average of the max temperature of SHA degradation and the max temperature of PZ degradation. Because it includes both amines, maximum temperatures are only listed in the above table for the initial, unbolded entries.

Figure 24 demonstrates the effect of CO_2 loading and acid loading on AMP and PZ degradation in 2.67 m AMP/1.33 m PZ.
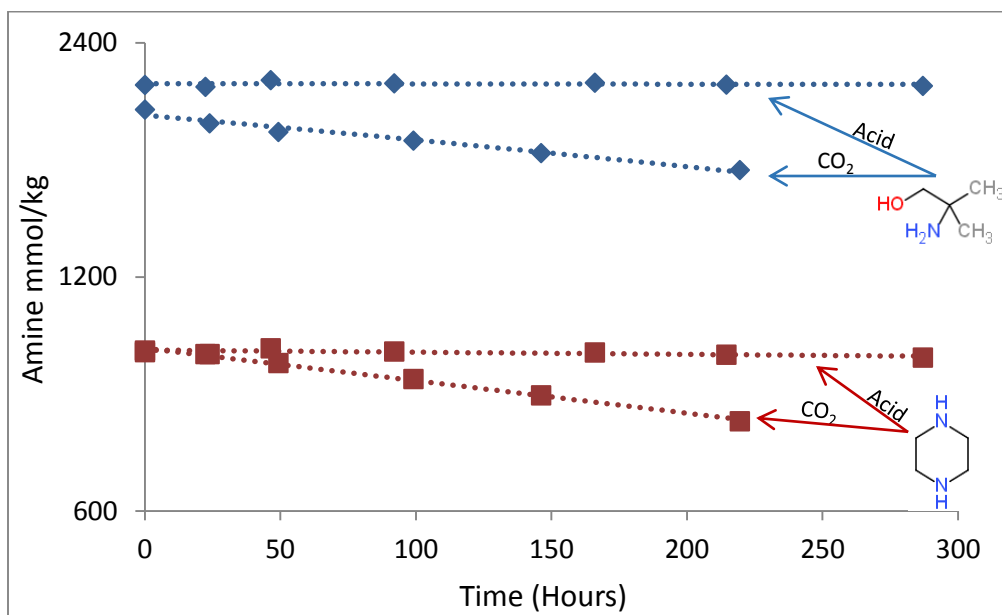
Fig. 24. Degradation of AMP and PZ in a 2.67 m AMP/1.33 m PZ blend at 165 ºC under CO_2 α = 0.22 or H^+ α = 0.22. The acid-loaded samples do not appreciably degrade.

The acid-loaded samples of AMP/PZ do not appreciably degrade at 165 ºC. AMP degrades with a reaction rate of 1.0e-5 hr^{-1} under these acidified conditions, compared to 76.3e-4 hr^{-1} under CO_2-loaded conditions. PZ degrades with a reaction rate of 6.3e-5 hr^{-1} under acidified conditions,

compared to 9.61e-4 hr^{-1} under CO_2-loaded conditions. This sharp drop in degradation rates from CO_2-loaded conditions to acid-loaded conditions suggests that the degradation mechanism requires and incorporates CO_2.

Corrosion

Results from this section are based on a previous report on corrosion (Carlson, Hatchell, Sirkar, 2015).

The ICP-OES measured concentrations in every cylinder for five metals: chromium, iron, manganese, molybdenum, and nickel. Every data point presented below as metal concentrations corresponds to a data point presented above as amine loss. Figures 25 and 26 display the accumulation of metals, and therefore the extent of corrosion, in the cylinders used for the MEA and MPA time series.
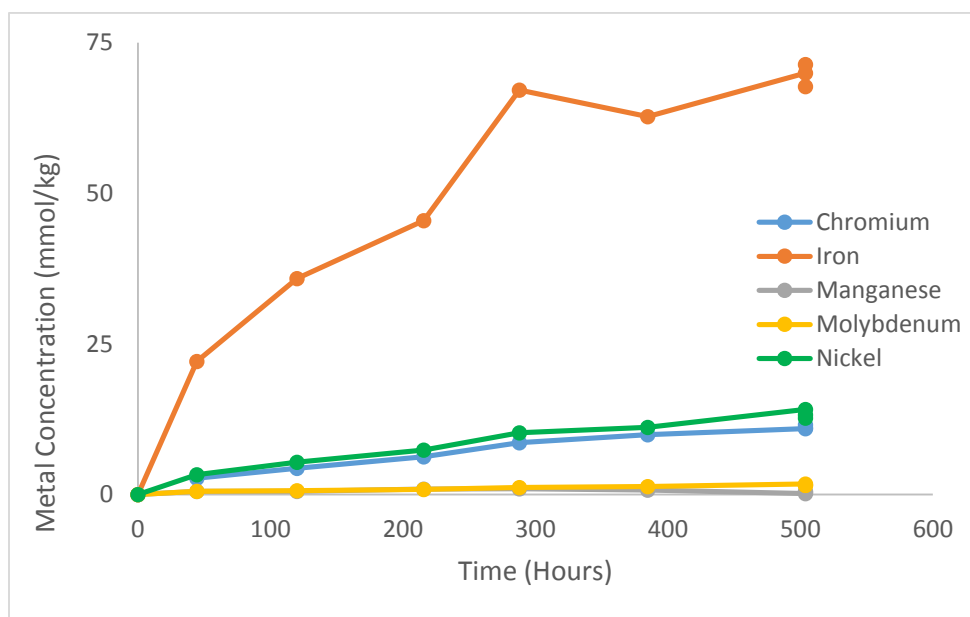
Fig. 25. Metal accumulation in MEA over three weeks. MEA maintained at 135 ºC, α = 0.35, and 10 m concentration.
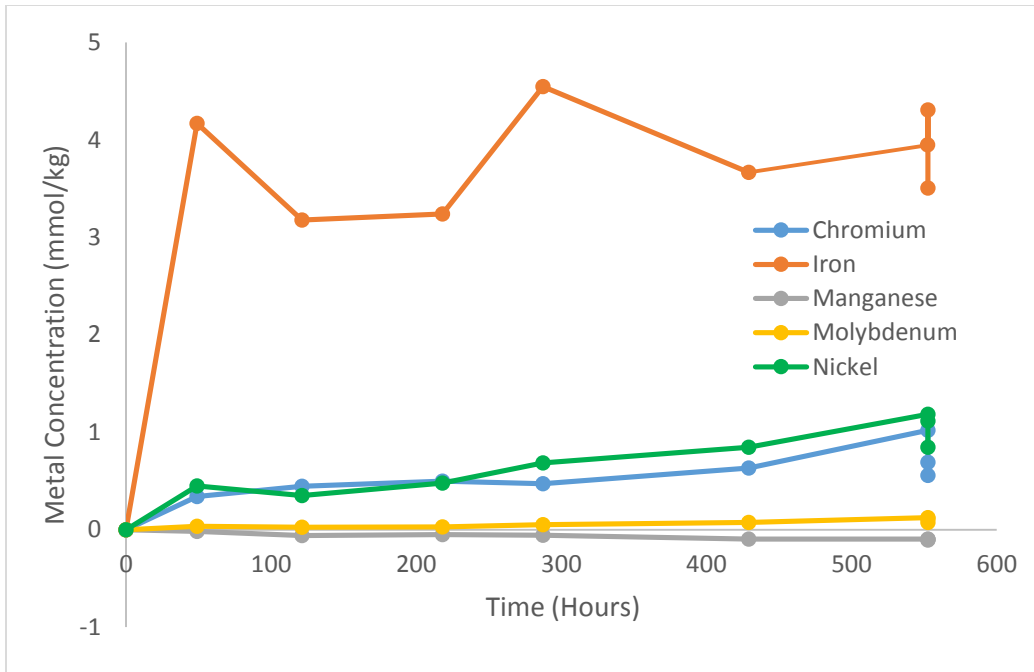
Fig. 26. Metal accumulation in MPA over three weeks. MPA maintained at 135 ℃, α = 0.35, and 10 m concentration.

The shape of the two plots are similar, although MEA concentrations are on average fifteen times greater than MPA concentrations. Figures 27 through 29 below display the effect of different process variables on metal accumulation in MEA. Figures 30 through 32 show the same effect for MPA. The plots only include iron concentrations; because the trends for all metals were similar, iron serves as a proxy for corrosion. Iron concentrations were the largest in MEA and MPA and should demonstrate the least additive error from the ICP.
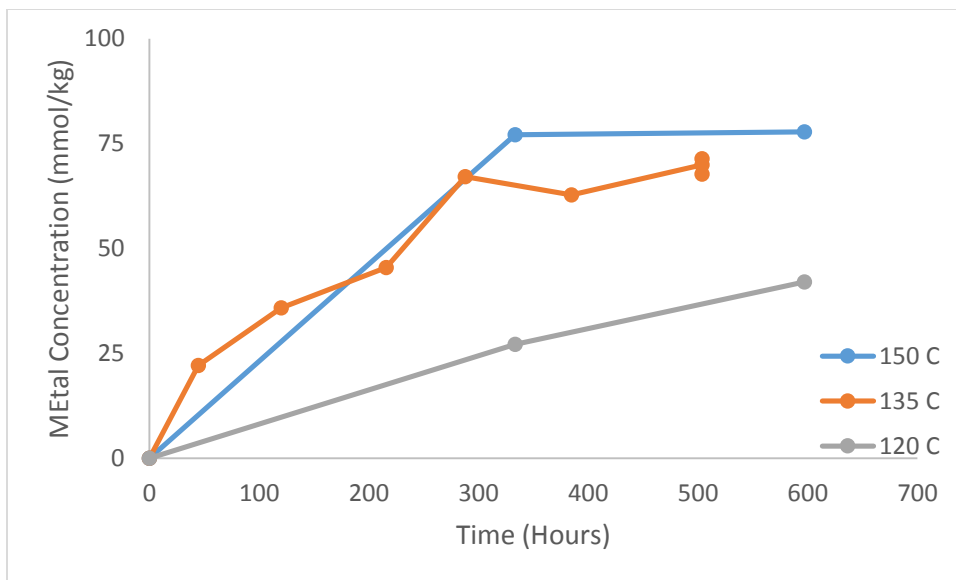
Fig. 27. Effect of temperature on iron accumulation in 10 m degrading MEA solutions. CO_2 loading is $\alpha = 0.35$.
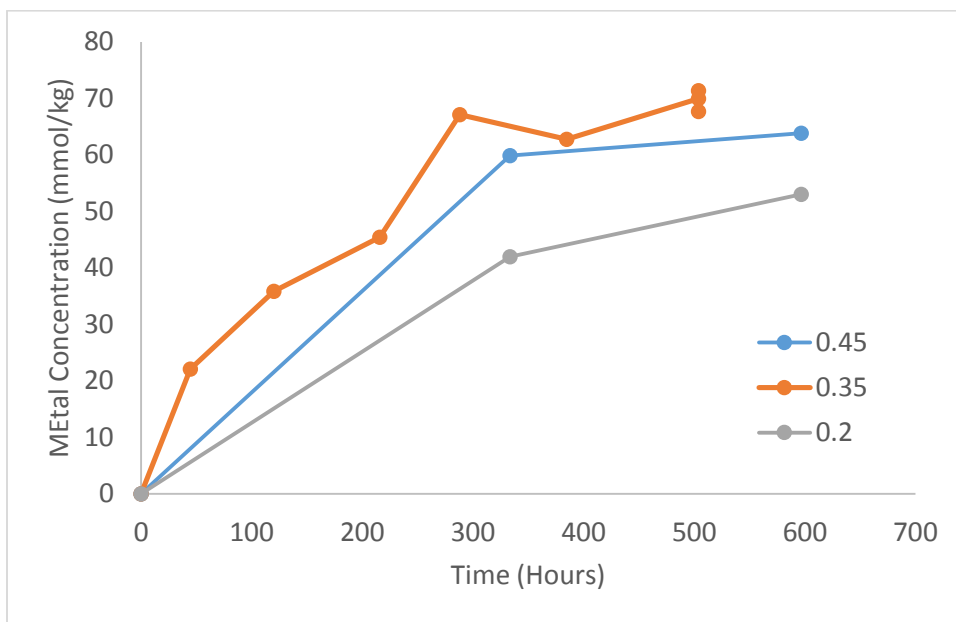
Fig. 28. Effect of CO_2 loading on iron accumulation in 10 m MEA solutions. Solutions maintained at 135 ºC.
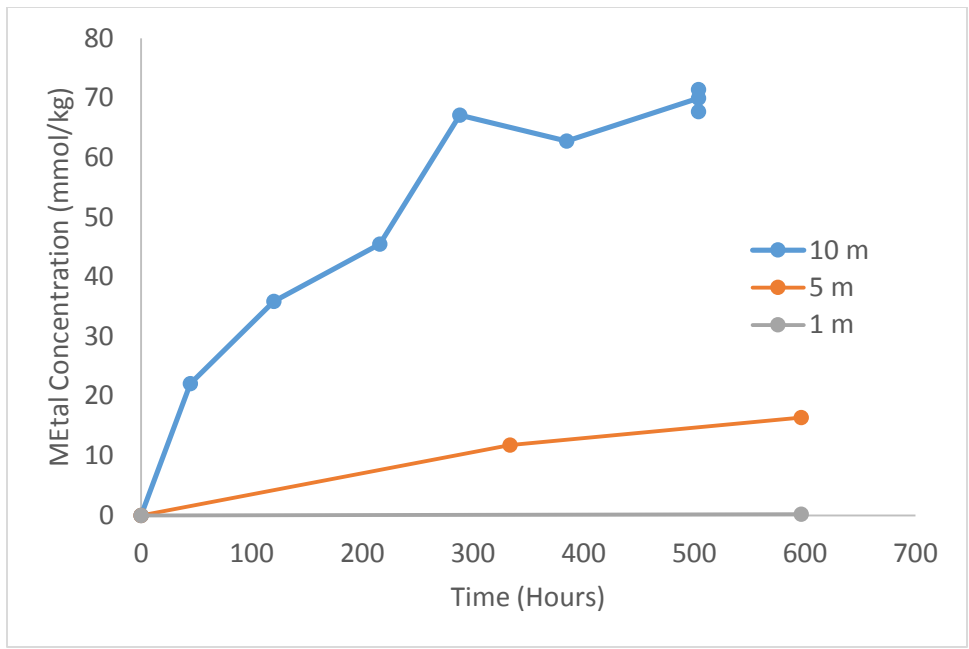
Fig. 29. Effect of amine concentration on iron accumulation in degrading MEA solutions. Solutions maintained at 135 ℃ and loaded with CO_2 to $\alpha = 0.35$.
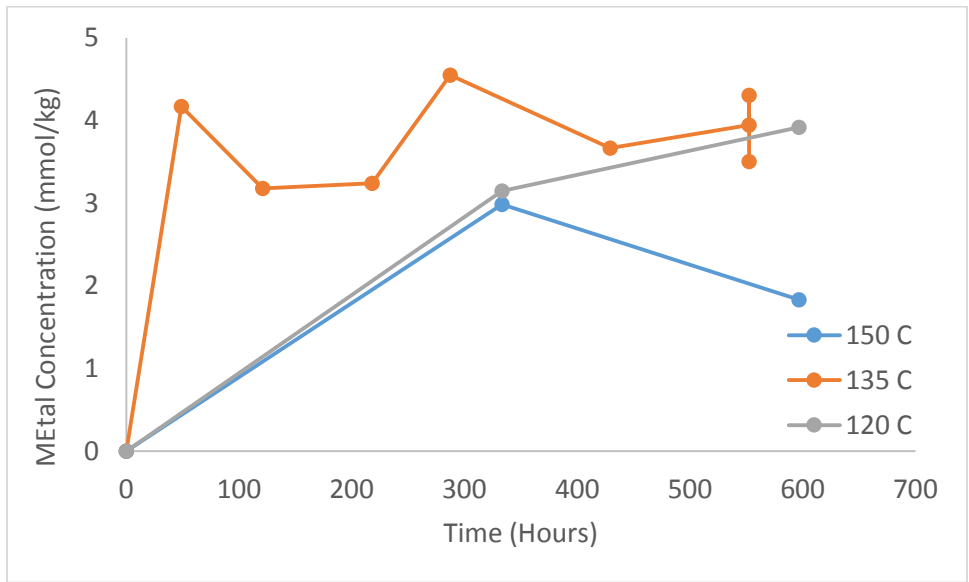
Fig. 30. Effect of temperature on iron accumulation in 10 m degrading MPA solutions. CO_2 loading is $\alpha = 0.35$.
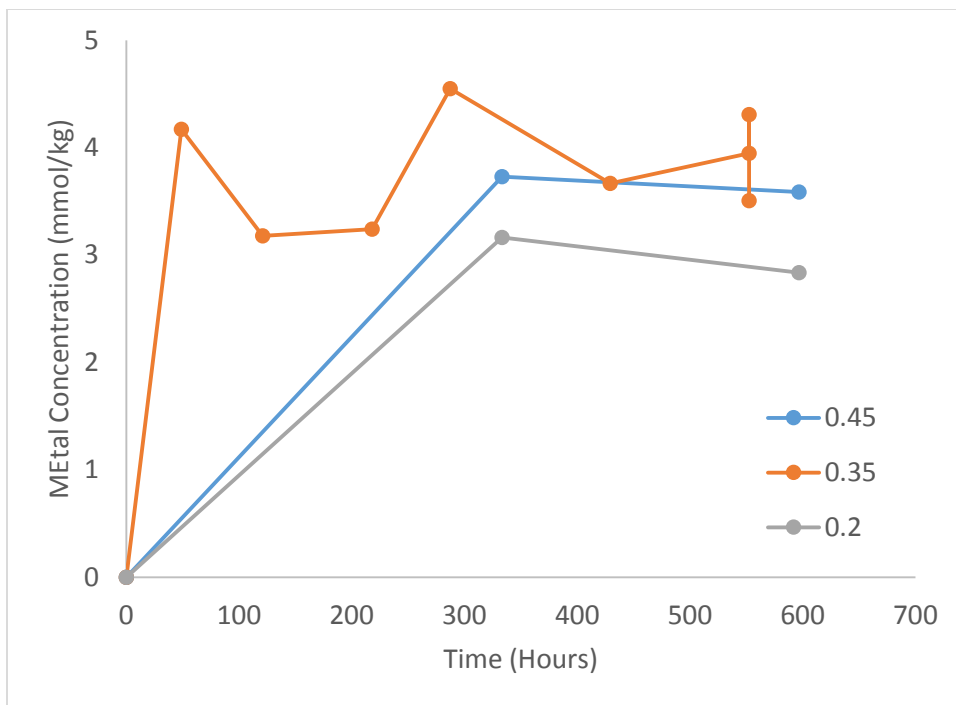
Fig. 31. Effect of CO_2 loading on iron accumulation in 10 m MPA solutions. Solutions maintained at 135 ℃.
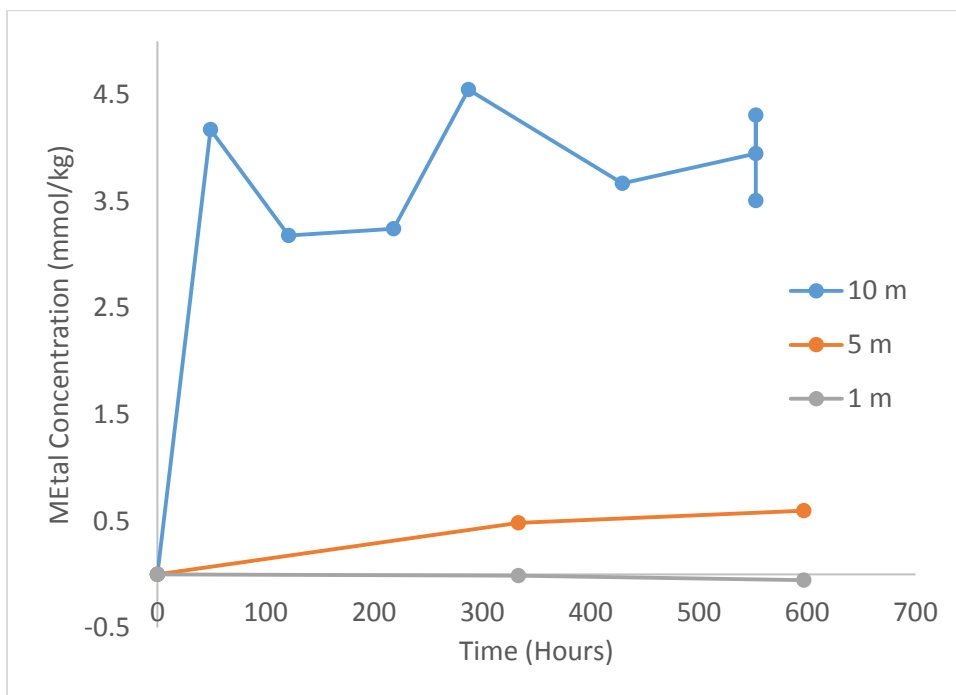
Fig. 32. Effect of amine concentration on iron accumulation in degrading MPA solutions. Solutions maintained at 135 ℃ and loaded with CO_2 to $\alpha = 0.35$.

Amine concentration affects corrosion more strongly than temperature or CO_2 loading. 10 m solutions dissolve metals at 1.5 to 6 times greater concentrations than 5 m solutions. This difference is present for every metal, except for manganese, where some of the concentrations are too low to accurately quantify with the ICP standard. Metals concentrations in the 10 m solutions are over 100 times greater than those of the 1 m solutions, although many of the measurements in the latter case also fall below the ICP standard and could not be measured accurately. The effects of CO_2 loading and temperature are more uncertain. The changes in corrosion caused by these two variables are too subtle to be identified within the error of this experiment.

Figure 33 presents a similar process variable study for EDA and PDA. This plot displays iron corrosion measurements for EDA and PDA after two weeks with variable concentration and CO_2 loading.
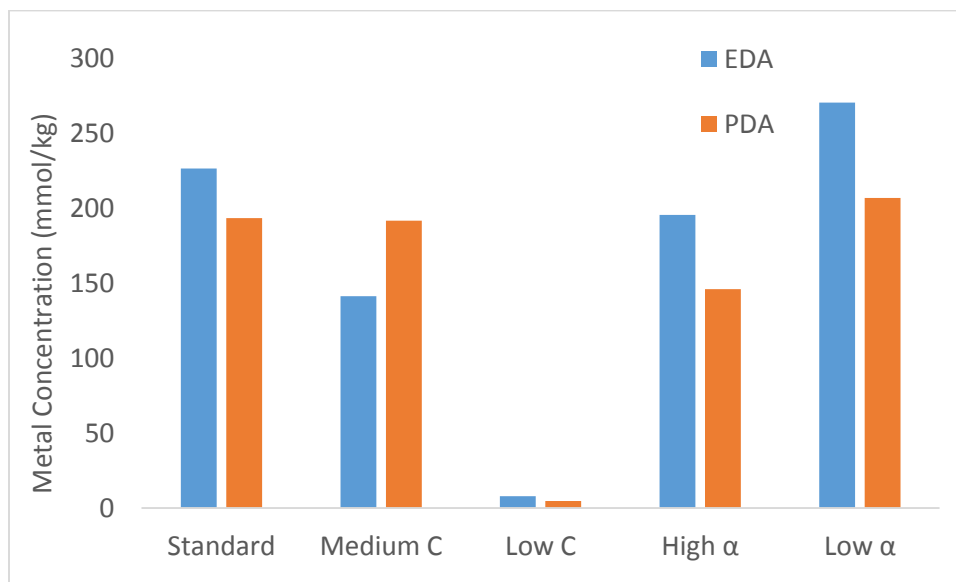
Fig. 33. Effect of concentration and loading on accumulation of iron in EDA and PDA solutions. Solutions were degraded at 135 ºC for two weeks (333 hours).

"Standard" conditions mimic the conditions of the MEA/MPA time series: 135 ºC, 10 m concentration, and CO_2 loading of $\alpha = 0.35$. "Medium C" and "Low C" refer to medium and low concentrations of 5 m and 1 m, respectively, while holding temperature and loading constant. "High α" and "Low α" refer to CO_2 loadings of $\alpha = 0.45$ and $\alpha = 0.2$, respectively, maintaining

standard conditions for temperature and concentration. Amine concentration again appears to strongly correlate with corrosion in the EDA solutions. This effect is less pronounced for PDA, possibly due to an error in the "Medium C" data point, the only point that is higher than its EDA counterpart. The effect of loading is not as large as that of concentration, but corrosion appears to increase as loading decreases.

EDA corrodes slightly more than PDA, although the difference is not nearly as great as that of MEA and MPA. Figure 34 below compares the corrosion of EDA and PDA for all five metals measured:
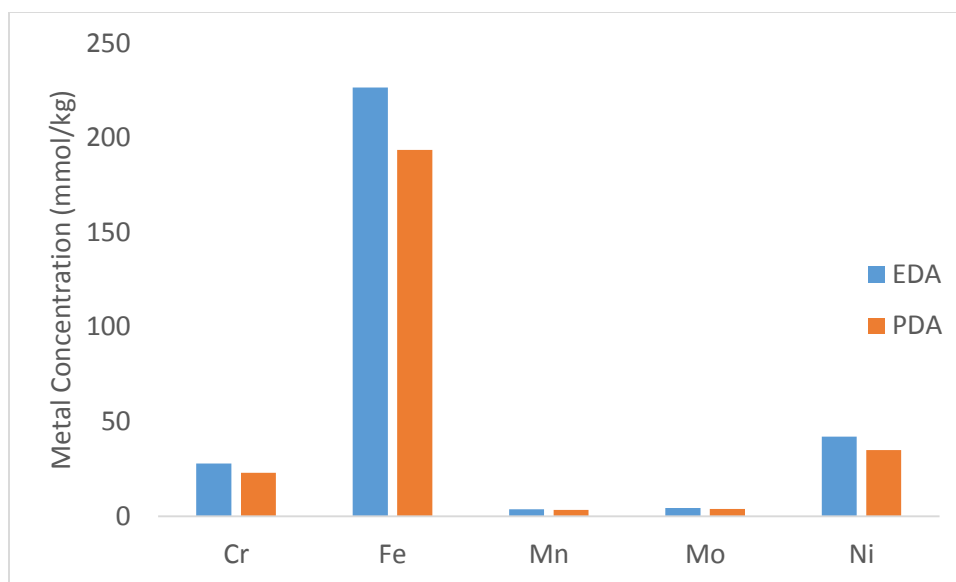
Fig. 34. Metal accumulation in EDA and PDA solutions. All solutions were prepared at 10 m amine concentration and a CO_2 loading of $\alpha = 0.35$. All solutions were degraded at 135 ℃ for two weeks (333 hours).

EDA is a fairly consistent 1.2 times more corrosive than PDA across all metals. Iron again appears to serve as a good proxy for general metals corrosion.

Figures 35 through 37 presents similar plots to Figure 34 comparing the corrosion of related compounds taken from the single point degradation studies. All data points represent degradation for 3.5 weeks (597 hours) at 135 ℃, although the loadings and concentrations are not necessarily

the same as the previously used standard conditions.
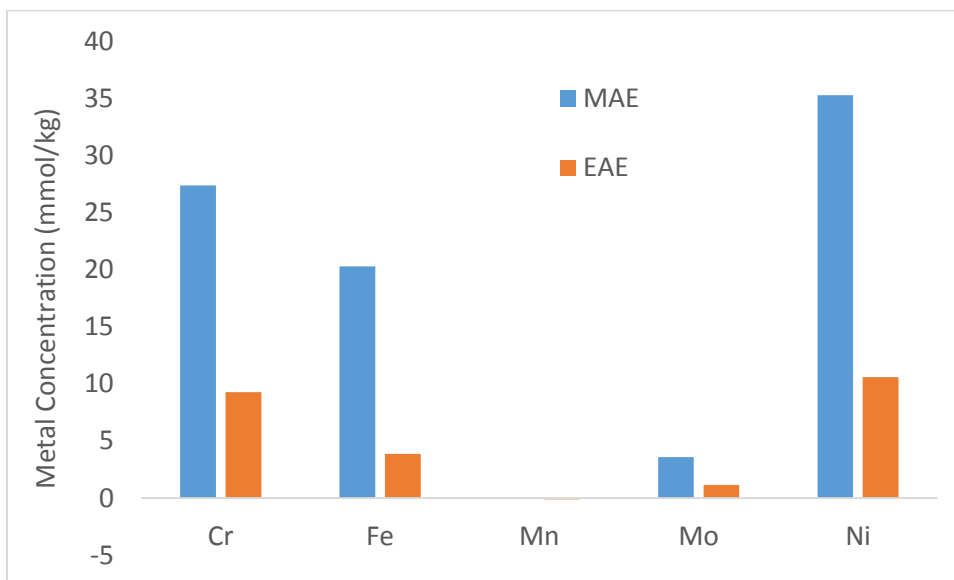
Fig. 35. Metal accumulation in MAE and EAE solutions. Solutions were prepared at 10 m amine concentration, α = 0.4, and 135 ℃. Manganese concentrations are very close to zero.
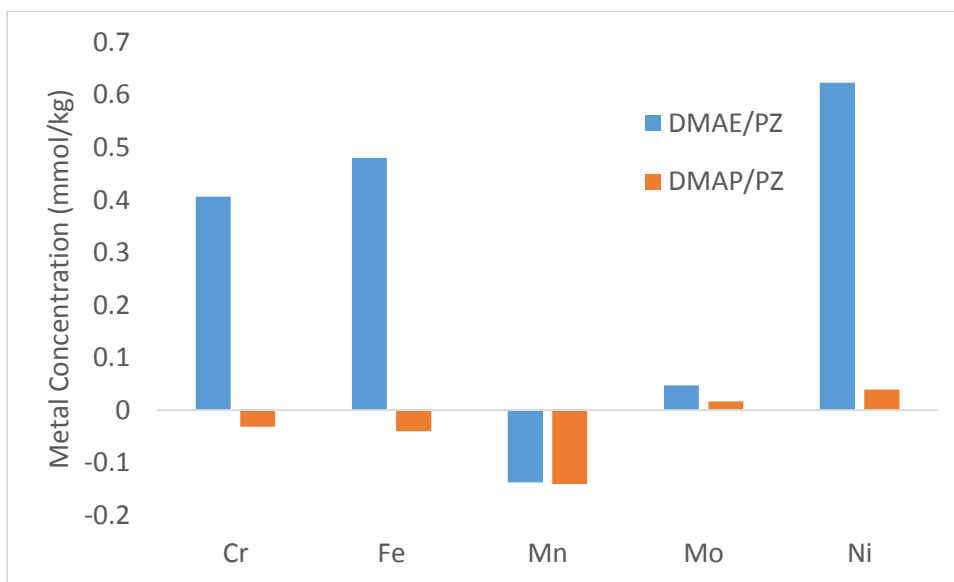
Fig. 36. Metal accumulation in DMAE/PZ and DMAP/PZ solutions. Solutions were prepared at 3.33 m amine and 3.33 m PZ concentration, α = 0.25, and 135 ℃. Negative metals measurements represent data below the ICP standard.
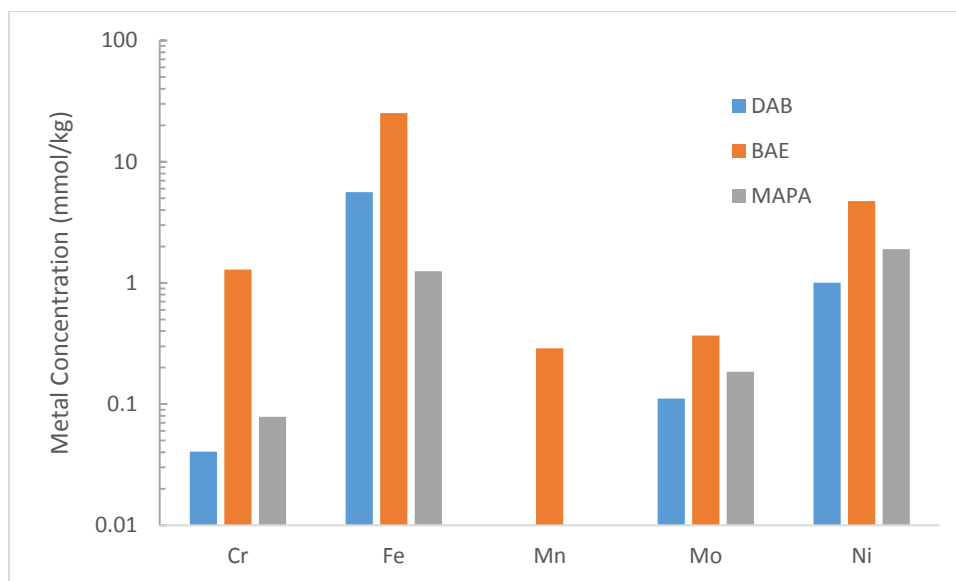
Fig. 37. Metal accumulation in DAB, BAE, and MAPA solutions. DAB and BAE solutions were prepared at 5 m amine concentration, α = 0.4, and 135 ℃. MAPA was prepared at α = 0.35 and 10 m. Although MAPA is more structurally related to PDA, the corrosivity is on a similar scale to BAE and DAB.

General corrosion comparisons can be made across the previous plots. MAE corrodes on average three times more than EAE; BAE corrodes five times more than DAB; PDA corrodes on average 120 times more than MAPA. The plot of DMAE/PZ and DMAP/PZ corrosion included too many negative metals values to give an accurate comparison, but DMAE/PZ clearly corrodes more quickly.

An earlier study tested for corrosion and formate concentration in EDA, PDA, DAB, and BAE (Fischer 2014). It was found that the concentration of formate and dissolved metals increased over time as some amines degraded in the metal cylinders. Figure 38 plots the concentration of formate in the samples of the four diamines as they degrade at 150 ℃ at 0.4 CO_2 loading.
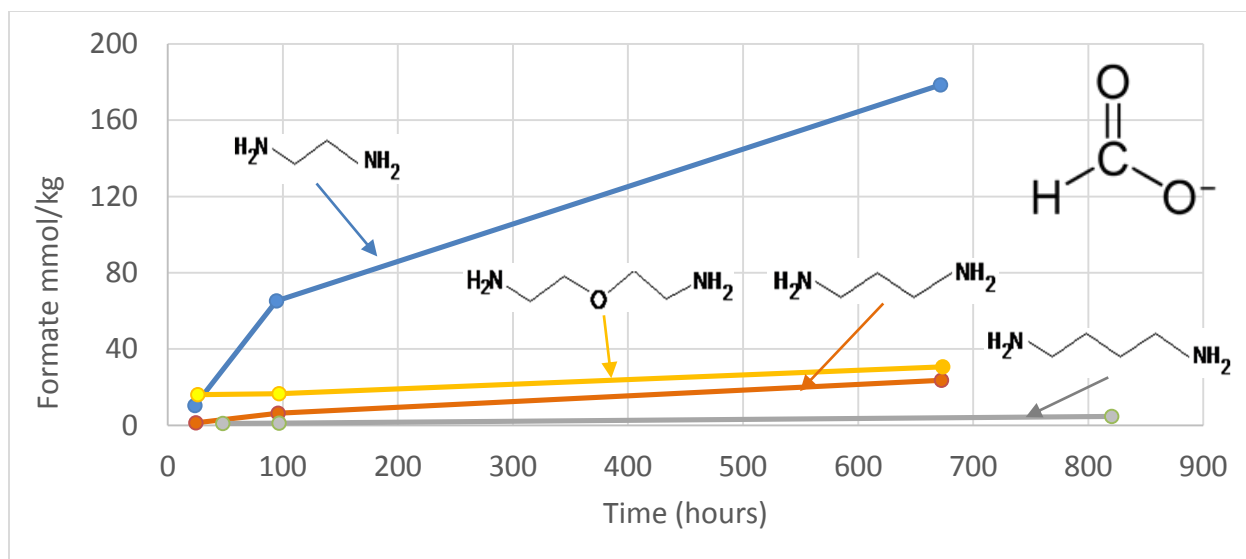
Fig. 38. Total formate generation in degraded 5 m EDA, 5 m PDA, 5 m DAB, and 5 m BAE. Samples degraded at 150 °C with CO_2 loading of 0.4.

Figure 39 displays the concentrations of chromium, nickel, manganese, and iron in the last of the degraded samples from the 150 °C series (this corresponds to 670 hours of degradation for EDA, PDA, and DAB, and 810 hours of degradation for BAE).
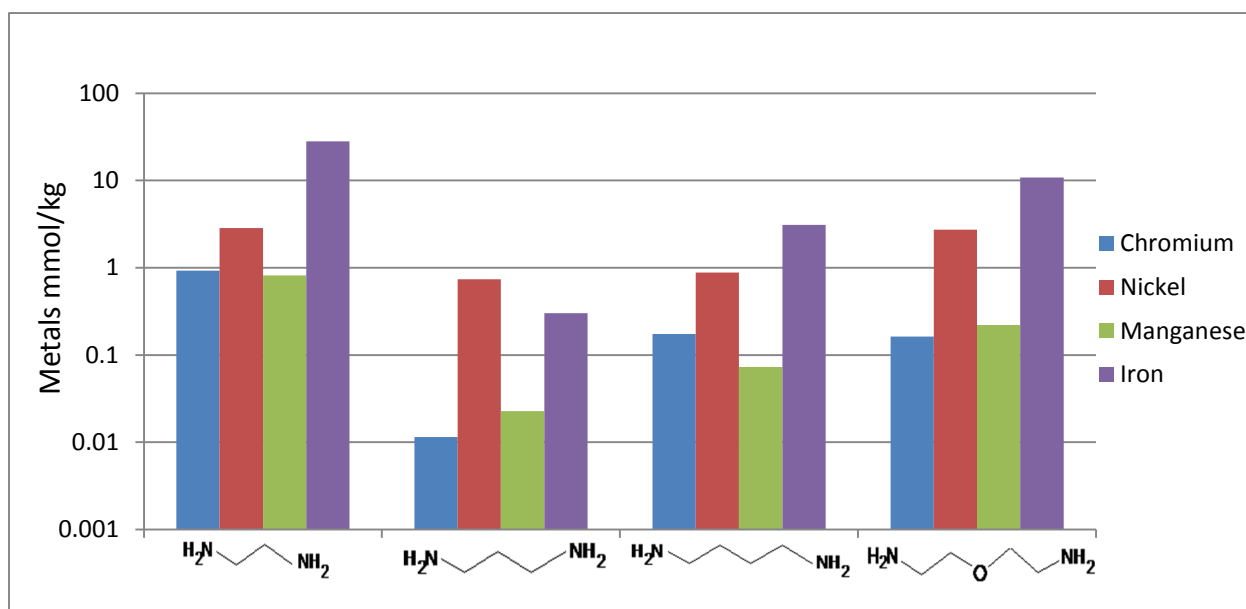
Fig. 39. Concentration of metals in the twelfth (last) amine sample of 150 °C, 0.4 CO_2 loading degradation series. Metals and formate are most prominent in EDA.

These two plots reveal a correlation in the concentration of heat-stable salts in solution and the concentration of corroded metals. EDA is especially corrosive and generates a large amount of formate while degrading, while DAB and PDA contain significantly less formate and metals in the degraded solution. These results have implications in oxidative degradation. Metals are known to catalyse the oxidative degradation of certain amines [6]. It is unknown whether the generation of heat-stable salts drives corrosion or if dissolved metals catalyse heat-stable salt formation. Describing this relationship may lead to a better understanding of how to identify compounds resistant to corrosion and oxidation.

There is a discrepancy, however, in the corrosion data of PDA from Figure 39 compared with Figures 33 and 34. The previous study (Figures 38 and 39) saw that PDA corroded 40 to 80 times less than EDA, supporting the two-carbon / three-carbon hypothesis. PDA and EDA were seen to corrode at similar rates in Figures 33 and 34, a contradiction. It is worth further investigating the corrosion of PDA to resolve this problem.

Conclusion

Maximum stripping temperature appears to correlate very strongly with amine chain length. The five diamines, in order of chain length, have the following max temperatures: EDA (116 °C), PDA (124 °C), DAB (126 °C), BAE (130 °C), and HMDA (140 °C). Alkanolamines in order of chain length are MEA (116 °C), MPA (129 °C), and DGA® (134 °C). The SHA/PZ blends have the following weighted max temperatures: AMP (143 °C), AMPD (135 °C), TRIS (130 °C), tBuAE (150 °C), PM (97 °C), and PE (129 °C). The linear amines tested follow either first-order or initial first-order degradation curves, corroborating the ring-closing mechanisms proposed in literature. Replacing CO_2 loading with acid loading significantly slows degradation rates of EDA, PDA, BAE, and AMP, suggesting that the degradation mechanisms incorporate CO_2. DAB degradation does not significantly slow with acid loading.

The two-carbon / three-carbon hypothesis of corrosion is supported by comparing metals data from MEA/MPA (15 times faster), MAE/EAE (3 times faster), and DMAE-PZ/DMAP-PZ (indeterminate but qualitatively faster), the two-carbon amine being faster in each case. Older data of EDA and PDA suggests that EDA corrodes 40 to 80 times faster (Figure 38), but more recent tests show similar corrosion rates where EDA is only 1.2 times faster (Figures 32 and 33). Corrosion appears to be a strong function of amine concentration, not varying significantly with changes in temperature of CO_2-loading. Corrosion also appears to correlate with the accumulation of formate in solution.

Future work should highlight some of the questions faced in this study; the discrepancy between PDA corrosion rates should be investigated again, and the role of formate should be examined for all of the alkanolamines and SHA/PZ blends. The degradation and corrosion of cadaverine should also be measured. Cadaverine would more accurately complete the set of diamines varying with structure, seeing that BAE was originally selected as a cheaper and more available alternative. The corrosion experiments could also be performed in carbon steel cylinders. Carbon steel is known to corrode more than stainless steel, but is cheaper and would significantly lower the price of an amine scrubber; amines that do not corrode carbon steel could be economically competitive scrubbing solvents.

References

Amine Based Post Combustion. [Electronic Image]. Retrieved from: <http://www.co2crc.com.au/aboutccs/cap_absorption.html>

Carlson, M.C., Hatchell, D.C., Sirkar, S. (2015) *Thermal Degradation and Corrosion of Amines*. CHE 264 Special Project Final Report. The University of Texas at Austin.

Davis, J.D. *Thermal Degradation of Aqueous Amines Used for Carbon Dioxide Capture*. The University of Texas at Austin. Ph.D. Dissertation. 2009.

Department of Energy. "Carbon Storage R&D" N.p., 2014. Web. 13 March 2015. <http://energy.gov/fe/science-innovation/carbon-capture-and-storage-research/carbon storage-rd>

Fischer, K. "Corrosivity Screening of Amine Solutions in Thermal Cylinders." Rochelle Group Fourth Quarterly Report, The University of Texas at Austin, Fall 2013.

Freeman SA. *Thermal Degradation and Oxidation of Aqueous Piperazine for Carbon Dioxide Capture.* The University of Texas at Austin. Ph.D. Dissertation. 2011.

Lepaumier H, Martin S, Picq D, Delfort B, Carrette P-L. "New Amines for CO_2 Capture. III. Effect of Alkyl Chain Length between Amine Functions on Polyamines Degradation." *Ind. Eng. Chem. Res.* 2010;49:4553–4560.

Namjoshi, O.A. *Thermal Degradation of PZ-Promoted Tertiary Amines for CO_2 Capture.* The University of Texas at Austin. Ph.D. Dissertation. 2015

Zhou S, Chen X, Nguyen T, Voice AK, Rochelle GT. "Aqueous Ethylenediamine for CO_2 Capture." *ChemSusChem*. 2010;3(8):913–918.

Appendix: Raw Data

Table 4: Degradation of diamines at 135 °C, α = 0.4, 10 m alkalinity. Times are listed in hours; concentrations are listed in mmol amine / kg solution.

EDA		PDA		DAB		BAE		HMDA	
Time	Conc.	Time	Conc.	Time	Conc.	Time	Conc.	Time	Conc.
0.0	3526.6	0.0	3318.8	0.0	3464.7	0.0	2815.9	0.0	1876.1
165.8	3185.8	165.8	3080.9	169.5	3077.7	169.5	2605.9	169.5	1827.8
306.3	2943.2	306.3	2921.2	337.2	2871.9	337.2	2511.4	337.2	1765.6
503.7	2485.4	503.7	2785.7	506.8	2704.3	506.8	2426.2	506.8	1769.2
666.8	2400.9	666.8	2621.3	671.9	2594.6	671.9	2388.3	671.9	1761.1
666.8	2417.3	666.8	2499.8	671.9	2633.0	671.9	2382.2	671.9	1770.9
666.8	2480.1	666.8	2513.7	671.9	2675.0	671.9	2386.7	671.9	1799.0
834.0	2389.1	834.0	2338.3	841.4	2556.8	841.4	2344.7	841.4	1769.7
1295.6	2228.1	1295.6	2128.7	1008.5	2431.0	1008.5	2341.6	1008.5	1758.9
				1176.1	2386.7	1176.1	2294.9	1176.1	1752.0

Table 5: Degradation of diamines at 150 °C, α = 0.4, 10 m alkalinity. Times are listed in hours; concentrations are listed in mmol amine / kg solution.

EDA		PDA		DAB		BAE		HMDA	
Time	Conc.	Time	Conc.	Time	Conc.	Time	Conc.	Time	Conc.
0.0	3413.9	0.0	3319.9	0.0	3084.4	0.0	3025.3	0.0	1858.8
23.7	3245.7	24.6	3118.0	47.9	2698.4	26.2	2809.5	23.9	1812.8
49.2	2974.0	48.2	2976.3	74.5	2541.5	48.9	2657.9	48.5	1756.5
71.5	2760.9	72.7	2858.6	96.9	2477.8	73.7	2575.9	71.7	1749.1
94.6	2588.2	95.8	2703.3	96.9	2478.4	96.7	2518.4	95.4	1717.8
94.6	2625.3	95.8	2700.6	96.9	2478.8	96.7	2520.5	95.4	1735.8
94.6	2655.7	95.8	2777.9	169.5	2254.1	96.7	2553.2	95.4	1740.2
167.5	2327.8	194.8	2393.1	241.5	2091.0	170.4	2460.1	167.7	1705.0
259.4	2100.3	240.7	2124.4	338.4	1846.5	242.3	2410.9	215.6	1717.5
335.4	1982.8	336.0	1922.0	504.3	1651.8	338.0	2377.3	335.5	1702.6
430.5	1936.2	431.5	1681.0	531.1	1639.4	433.7	2356.7	431.8	1675.2
527.6	1837.9	528.8	1448.6	675.3	1446.7	524.4	2367.6	528.6	1687.9
671.7	1808.7	672.3	1228.6	820.4	1308.1	673.7	2325.6	693.8	1663.0

Table 5: Degradation of diamines at 165 °C, α = 0.4, 10 m alkalinity. Times are listed in hours; concentrations are listed in mmol amine / kg solution.

EDA		PDA		DAB		BAE		HMDA	
Time	Conc.	Time	Conc.	Time	Conc.	Time	Conc.	Time	Conc.

0.0	3601.0	0.0	3254.7	0.0	3186.1	0.0	2977.2	0.0	1914.5
24.4	2995.5	24.4	2710.4	24.4	2410.4	24.4	2383.0	24.4	1792.8
48.0	2501.2	48.0	2400.2	48.0	2139.3	48.0	2322.3	48.0	1730.3
72.0	2190.3	72.0	1978.3	72.0	1919.6	72.0	2256.3	72.0	1686.8
96.4	2019.3	96.4	1853.3	96.4	1736.4	96.4	2236.3	96.4	1677.3
119.9	1850.4	119.9	1453.5	119.9	1635.8	119.9	2213.1	119.9	1676.5

Table 7: Degradation of alkanolamines at 135 °C, α = 0.4, 10 m alkalinity. Times are listed in hours; concentrations are listed in mmol amine / kg solution.

MEA		MPA		DGA	
Time	Conc.	Time	Conc.	Time	Conc.
0.0	6243.2	0.0	4634.7	0.0	3576.8
169.5	5366.0	169.5	4348.9	169.5	3337.4
337.2	4711.3	337.2	4258.5	337.2	3265.1
506.8	4004.5	506.8	4136.0	506.8	3203.4
671.9	3517.5	671.9	4015.8	671.9	3139.0
671.9	3523.0	671.9	4072.8	671.9	3249.8
671.9	3585.9	671.9	3984.4	671.9	3191.6
841.4	3060.3	841.4	3951.7	841.4	3228.4
1008.5	2644.1	1008.5	3742.4	1008.5	3058.5
1176.1	2257.4	1176.1	3633.4	1176.1	3035.9

Table 8: Degradation of alkanolamines at 150 °C, α = 0.4, 10 m alkalinity. Times are listed in hours; concentrations are listed in mmol amine / kg solution.

MEA		MPA		DGA	
Time	Conc.	Time	Conc.	Time	Conc.
0.0	5600.7	0.0	5267.3	0.0	4659.6
24.2	5172.4	24.8	5057.9	24.2	4443.7
47.2	4811.2	47.7	4904.1	47.2	4265.6
72.6	4458.8	72.2	4810.9	72.6	4200.2
95.6	4058.2	93.3	4708.4	95.6	4049.3
95.6	4062.1	93.3	4714.9	95.6	4113.4
95.6	4120.4	93.3	4666.4	95.6	4066.3
168.1	3230.6	167.7	4464.0	168.1	3964.4
264.5	2434.3	241.0	4281.3	264.5	3915.1
357.5	1909.4	336.5	3974.8	357.5	3915.4
503.7	1333.9	432.9	3704.8	503.7	3893.5
527.9	1190.8	528.1	3451.2	527.9	3877.8
670.4	847.3	672.1	2891.6	670.4	3859.7
670.4	1020.0			670.4	3862.0

Table 9: Degradation of alkanolamines at 165 °C, α = 0.4, 10 m alkalinity. Times are listed in hours; concentrations are listed in mmol amine / kg solution.

MEA		MPA		DGA	
Time	Conc.	Time	Conc.	Time	Conc.
0.0	5599.4	0.0	5308.8	0.0	4691.2
24.2	4244.3	24.2	4657.6	24.2	4104.2
48.3	3414.9	48.3	4466.9	48.3	3987.6
72.0	2699.6	72.0	4177.6	72.0	3839.7
95.7	2196.8	95.7	3929.0	95.7	3912.3
119.9	1757.7	119.9	3679.2	119.9	3840.9

Table 10: Degradation of diamines at 165 °C, α = 0.2, 10 m alkalinity (acid loaded). Times are listed in hours; concentrations are listed in mmol amine / kg solution.

EDA		PDA		DAB		BAE	
Time	Conc.	Time	Conc.	Time	Conc.	Time	Conc.
0.0	2287.5	0.0	2046.0	0.0	2068.1	0.0	2116.2
24.4	2243.0	24.4	2008.3	24.4	1765.0	24.4	2107.3
48.0	2050.3	48.0	2039.6	48.0	1569.3	48.0	2094.5
72.0	2018.0	72.0	1965.8	72.0	1427.1	72.0	2106.9
96.4	1993.1	96.4	1928.6	96.4	1270.9	96.4	2054.3
119.9	1940.5	119.9	1882.0	119.9	1155.5	119.9	2090.2

Table 11: Degradation of hindered amine blends at 135 °C, α = 0.22, 2.67/1.33 m alkalinity. Times are listed in hours; concentrations are listed in mmol amine / kg solution. Amine values are listed first; piperazine values are listed second, bolded.

AMP		AMPD		TRIS		tBuAE		PM		PE	
Time	Conc.	Time	Conc.	Time	Conc.	Time	Conc.	Time	Conc.	Time	Conc.
0.0	1992.3	0.0	1898.3	0.0	1905.6	0.0	1968.0	0.0	2011.1	0.0	1873.6
172.0	1998.0	172.0	1708.3	172.0	1688.6	172.0	1944.2	172.0	1231.7	172.0	1807.4
337.6	1968.6	337.6	1677.5	337.6	1789.5	337.6	1931.1	337.6	744.3	337.6	1751.7
509.3	1942.2	509.3	1626.1	509.3	1636.4	509.3	1917.0	509.3	475.2	509.3	1675.0
695.4	1908.4	695.4	1573.9	695.4	1647.5	695.4	1911.6	695.4	296.4	695.4	1624.1
838.7	1906.5	838.7	1538.8	838.7	1570.5	838.7	1902.4	838.7	233.8	838.7	1595.1
1012.0	1892.4	1012.0	1486.5	1012.0	1550.5	1012.0	1895.8	1012.0	185.3	1012.0	1529.9
0.0	**951.8**	**0.0**	**938.2**	**0.0**	**908.0**	**0.0**	**923.2**	**0.0**	**900.9**	**0.0**	**898.7**
172.0	**960.5**	**172.0**	**934.7**	**172.0**	**881.3**	**172.0**	**916.6**	**172.0**	**481.2**	**172.0**	**872.2**
337.6	**953.3**	**337.6**	**935.2**	**337.6**	**861.1**	**337.6**	**908.6**	**337.6**	**261.6**	**337.6**	**842.3**
509.3	**934.6**	**509.3**	**936.5**	**509.3**	**823.8**	**509.3**	**896.6**	**509.3**	**164.5**	**509.3**	**802.5**
695.4	**911.7**	**695.4**	**930.6**	**695.4**	**800.1**	**695.4**	**888.5**	**695.4**	**108.8**	**695.4**	**777.8**

838.7	910.1	838.7	921.4	838.7	765.3	838.7	883.6	838.7	92.5	838.7	761.7
1012.0	894.9	1012.0	914.2	1012.0	737.5	1012.0	878.0	1012.0	78.2	1012.0	726.7

Table 12: Degradation of hindered amine blends at 150 °C, α = 0.22, 2.67/1.33 m alkalinity. Times are listed in hours; concentrations are listed in mmol amine / kg solution. Amine values are listed first; piperazine values are listed second, bolded.

AMP		AMPD		TRIS		tBuAE		PM		PE	
Time	Conc.	Time	Conc.	Time	Conc.	Time	Conc.	Time	Conc.	Time	Conc.
0.0	1830.3	0.0	1764.5	0.0	1751.1	0.0	1843.0	0.0	2013.8	0.0	1830.3
25.8	1762.1	25.8	1585.7	25.8	1554.8	25.8	1994.1	25.8	1524.1	25.8	1762.1
48.8	1696.9	48.8	1595.0	48.8	1573.5	48.8	1941.1	48.8	1244.5	48.8	1696.9
72.2	1701.1	72.2	1572.6	72.2	1512.1	72.2	1908.9	72.2	983.0	72.2	1701.1
96.5	1674.4	96.5	1494.4	96.5	1635.3	96.5	1891.2	96.5	839.5	96.5	1674.4
96.5	1674.3	96.5	1547.8	96.5	1549.5	96.5	1900.4	96.5	796.0	96.5	1674.3
96.5	1678.5	96.5	1494.2	96.5	1555.4	96.5	1851.1	96.5	803.5	96.5	1678.5
167.8	1589.0	167.8	1524.2	167.8	1562.9	167.8	2033.1	167.8	447.6	167.8	1589.0
239.1	1548.5	239.1	1369.6	239.1	1547.8	239.1	1897.5	239.1	303.3	239.1	1548.5
336.3	1426.9	336.3	1437.6	336.3	1422.8	336.3		336.3	184.3	336.3	1426.9
431.8	1519.8	431.8	1251.7	431.8	1396.8	431.8	1869.8	431.8	144.2	431.8	1519.8
527.8	1286.2	527.8	1316.3	527.8	1442.7	527.8	1865.0	527.8		527.8	1286.2
695.6	1180.5	695.6	1118.9	695.6	1343.4	695.6	1835.8	695.6		695.6	1180.5
0.0	**889.5**	**0.0**	**924.1**	**0.0**	**901.6**	**0.0**	**881.4**	**0.0**	**866.8**	**0.0**	**889.5**
25.8	**879.7**	**25.8**	**932.3**	**25.8**	**869.8**	**25.8**	**942.5**	**25.8**	**632.1**	**25.8**	**879.7**
48.8	**836.7**	**48.8**	**938.3**	**48.8**	**873.1**	**48.8**	**921.0**	**48.8**	**485.6**	**48.8**	**836.7**
72.2	**839.2**	**72.2**	**959.1**	**72.2**	**832.8**	**72.2**	**898.9**	**72.2**	**362.9**	**72.2**	**839.2**
96.5	**824.1**	**96.5**	**932.5**	**96.5**	**864.1**	**96.5**	**894.2**	**96.5**	**303.3**	**96.5**	**824.1**
96.5	**820.9**	**96.5**	**930.2**	**96.5**	**840.7**	**96.5**	**895.4**	**96.5**	**286.2**	**96.5**	**820.9**
96.5	**821.5**	**96.5**	**925.6**	**96.5**	**842.2**	**96.5**	**872.4**	**96.5**	**289.4**	**96.5**	**821.5**
167.8	**776.6**	**167.8**	**940.3**	**167.8**	**815.7**	**167.8**	**949.3**	**167.8**	**161.0**	**167.8**	**776.6**
239.1	**746.9**	**239.1**	**910.9**	**239.1**	**783.4**	**239.1**	**884.0**	**239.1**	**117.3**	**239.1**	**746.9**
336.3	**690.6**	**336.3**	**927.8**	**336.3**	**725.1**	**336.3**		**336.3**	**84.6**	**336.3**	**690.6**
431.8	**726.4**	**431.8**	**867.5**	**431.8**	**682.2**	**431.8**	**848.9**	**431.8**	**78.6**	**431.8**	**726.4**
527.8	**618.5**	**527.8**	**889.5**	**527.8**	**688.0**	**527.8**	**844.3**	**527.8**		**527.8**	**618.5**
695.6	**565.6**	**695.6**	**804.8**	**695.6**	**570.4**	**695.6**	**815.3**	**695.6**		**695.6**	**565.6**

Table 13: Degradation of hindered amine blends at 165 °C, α = 0.22, 2.67/1.33 m alkalinity. Times are listed in hours; concentrations are listed in mmol amine / kg solution. Amine values are listed first; piperazine values are listed second, bolded.

AMP		AMPD		TRIS		tBuAE		PM		PE	
Time	Conc.	Time	Conc.	Time	Conc.	Time	Conc.	Time	Conc.	Time	Conc.

0.0	1971.6	0.0	1700.2	0.0	1826.7	0.0	1964.5	0.0	2056.1	0.0	1682.6
23.9	1892.6	23.9	1486.6	23.9	1553.7	23.9	1943.7	23.9	1118.0	23.9	1736.8
49.3	1844.6	49.3	1469.5	49.3	1565.5	49.3	1924.9	49.3	603.8	49.3	1671.3
99.1	1797.8	99.1	1341.3	99.1	1489.9	99.1	1920.6	99.1	258.2	99.1	1495.0
146.2	1732.4	146.2	1269.4	146.2	1385.7	146.2	1892.0	146.2	170.4	146.2	1365.3
219.6	1648.5	219.6	1113.7	219.6	1286.1	219.6	1838.9	219.6	124.6	219.6	1173.3
0.0	**960.7**	**0.0**	**869.0**	**0.0**	**874.6**	**0.0**	**916.8**	**0.0**	**904.3**	**0.0**	**831.2**
23.9	**955.4**	**23.9**	**863.3**	**23.9**	**833.9**	**23.9**	**903.3**	**23.9**	**443.5**	**23.9**	**830.5**
49.3	**930.3**	**49.3**	**872.9**	**49.3**	**796.9**	**49.3**	**887.1**	**49.3**	**228.0**	**49.3**	**792.6**
99.1	**887.9**	**99.1**	**855.0**	**99.1**	**735.8**	**99.1**	**875.6**	**99.1**	**118.3**	**99.1**	**700.2**
146.2	**845.5**	**146.2**	**826.2**	**146.2**	**647.6**	**146.2**	**853.2**	**146.2**	**99.0**	**146.2**	**638.2**
219.6	**783.3**	**219.6**	**788.9**	**219.6**	**542.3**	**219.6**	**816.4**	**219.6**	**96.5**	**219.6**	**550.5**

Table 14: Degradation of 4 m AMP / 2 m PZ at various temperatures, α = 0.22. Times are listed in hours; concentrations are listed in mmol amine / kg solution. First column in each temperature is the amine concentration; second is the piperazine concentration.

135 °C			150 °C			165 °C		
Time	Conc.		Time	Conc.		Time	Conc.	
0.0	2497.2	1284.0	0.0	2519.1	1281.1	0.0	2502.9	1290.6
168.5	2415.9	1269.4	23.3	2432.6	1264.3	23.6	2372.5	1277.5
358.7	2387.0	1247.7	48.9	2432.1	1274.2	49.1	2301.8	1223.7
503.4	2372.7	1236.0	72.6	2408.7	1261.4	72.8	2256.1	1194.5
673.3	2374.5	1230.2	95.8	2378.2	1248.4	96.1	2185.9	1149.2
837.9	2317.3	1194.1	95.8	2378.4	1245.2	120.6	2146.9	1114.8
1031.3	2315.3	1191.0	95.8	2386.6	1253.7			
			168.5	2332.0	1215.7			
			261.8	2276.1	1174.5			
			358.7	2242.0	1149.3			
			456.1	2212.5	1120.7			
			673.3	2095.5	1048.3			
			837.9	2042.9	1004.8			

Table 15. Metals concentrations in mmol / kg solution. The condition listed refers to the conditions explained in the above results section.

#	Amine	Condition	Cr	Fe	Mn	Mo	Ni
DL01	MEA	Standard	2.709525	22.09756	0.497309	0.502337	3.272679
DL02	MEA	Standard	4.320105	35.85551	0.524198	0.605702	5.337484
DL03	MEA	Standard	6.280978	45.45909	0.896712	0.839214	7.362089
DL04	MEA	Standard	8.571426	67.11314	0.937285	1.172927	10.26575
DL05	MEA	Standard	9.907128	62.74665	0.753747	1.341665	11.16702
DL06	MEA	Standard	10.95471	69.94339	0.16876	1.738362	14.11128
DL07	MEA	Standard	11.57873	71.39811	0.42594	1.517745	13.21298
DL08	MEA	Standard	11.05591	67.70504	0.442156	1.511509	12.70258

DL09	MPA	Standard	0.339601	4.171386	-0.01562	0.036495	0.450474
DL10	MPA	Standard	0.44461	3.178873	-0.05806	0.024294	0.349672
DL11	MPA	Standard	0.49831	3.241429	-0.04937	0.030466	0.480254
DL12	MPA	Standard	0.472044	4.548382	-0.05559	0.053151	0.686601
DL13	MPA	Standard	0.632951	3.668917	-0.09397	0.076586	0.845435
DL14	MPA	Standard	1.019608	3.947425	-0.09518	0.123323	1.184387
DL15	MPA	Standard	0.691839	4.307938	-0.1059	0.114873	1.114535
DL16	MPA	Standard	0.557235	3.506609	-0.09942	0.075385	0.845397
DL17	MEA	T+	5.332966	77.07995	0.009028	2.214664	26.90312
DL18	MEA	T+	2.027393	77.76658	-0.02956	1.627551	33.78883
DL19	MEA	T-	3.810582	27.18397	0.620659	0.47502	4.474843
DL20	MEA	T-	5.779642	42.02478	0.617437	0.793985	6.898675
DL21	MEA	C-	3.67761	11.80891	-0.08875	0.765556	6.649468
DL22	MEA	C-	4.326362	16.38683	-0.08825	1.032673	9.170705
DL24	MEA	C--	0.080953	0.222987	-0.1404	0.172294	1.552859
DL25	MEA	α+	12.82932	59.88126	0.14832	1.872805	16.37402
DL26	MEA	α+	14.12379	63.82571	0.080983	2.129481	18.63035
DL27	MEA	α-	4.908106	41.99831	0.951903	0.728886	6.366343
DL28	MEA	α-	3.530404	53.00496	1.291402	1.163582	10.08603
DL29	MPA	T+	0.857554	2.984615	-0.12094	0.168714	1.34351
DL30	MPA	T+	0.468832	1.833304	-0.12265	0.278304	1.795616
DL31	MPA	T-	0.381617	3.14779	-0.03517	0.021847	0.320864
DL32	MPA	T-	0.266468	3.91973	-0.00649	0.020376	0.453545
DL33	MPA	C-	0.093722	0.484288	-0.13528	0.007746	0.236748
DL34	MPA	C-	0.22445	0.598297	-0.13648	0.02853	0.400377
DL35	MPA	C--	-0.02943	-0.01339	-0.1378	-0.04518	-0.06109
DL36	MPA	C--	-0.02284	-0.05472	-0.14018	-0.02807	-0.04988
DL37	MPA	α+	0.806318	3.728652	-0.05346	0.068361	0.744316
DL38	MPA	α+	1.251092	3.58808	-0.08928	0.149367	1.275558
DL39	MPA	α-	0.257774	3.165242	0.04202	0.009582	0.289493
DL40	MPA	α-	0.207457	2.836115	-0.05162	0.042933	0.576849
DL41	EDA	C-	3.6164	141.4533	0.332219	1.813433	47.46618
DL42	EDA	C--	0.134152	7.854363	-0.13272	0.504201	21.82087
DL43	EDA	α+	26.49943	195.5606	3.312211	3.868224	36.83217
DL44	EDA	α-	40.36037	270.6768	6.211177	6.025726	55.67621
DL45	PDA	C-	27.57238	191.7384	3.392939	3.815394	34.73534
DL46	PDA	C--	0.344797	4.669958	-0.08056	0.079003	0.596081
DL47	PDA	α+	20.30061	146.1583	2.841472	2.884099	27.04142
DL48	PDA	α-	29.91702	207.0423	5.013385	3.990352	38.71781
DL49	EDA	Standard	27.79664	226.6127	3.626369	4.396149	41.98911
DL50	PDA	Standard	22.90253	193.5319	3.326689	3.815999	34.96485
DL51	MAE	Standard	27.3931	20.30399	-0.00521	3.600502	35.29397
DL52	EAE	Standard	9.276915	3.872557	-0.10039	1.160139	10.60118

DL53	DAB	Standard	0.040536	5.593282	-0.00683	0.111317	1.00699
DL54	BAE	Standard	1.285182	25.17231	0.288989	0.36844	4.738642
DL55	MAPA	Standard	0.078577	1.250951	-0.13579	0.185801	1.899926
DL56	DMAE/PZ	Standard	0.406319	0.479822	-0.13735	0.047032	0.623155
DL57	DMAP/PZ	Standard	-0.03123	-0.04005	-0.14034	0.016563	0.039498